Journal of Medicinal Chemistry

Article

Cite This: J. Med. Chem. 2019, 62, 5312−5329

pubs.acs.org/jmc

Design, Synthesis, and Biological Evaluation of a New Series of Carvedilol Derivatives That Protect Sensory Hair Cells from Aminoglycoside-Induced Damage by Blocking the Mechanoelectrical Transducer Channel

Molly O'Reilly,[†,⊥] Nerissa K. Kirkwood,[†,⊥] Emma J. Kenyon,[†] Rosemary Huckvale,[‡] Daire M. Cantillon,[§] Simon J. Waddell,[§] Simon E. Ward,[‡,∥] Guy P. Richardson,[†] Corné J. Kros,[†] and Marco Derudas*[,‡]

[†]Sussex Neuroscience, School of Life Sciences, and [‡]Sussex Drug Discovery Centre, School of Life Sciences, University of Sussex, Falmer, Brighton BN1 9QJ, U.K.

[§]Wellcome Trust Centre for Global Health Research, Brighton and Sussex Medical School, University of Sussex, Falmer, Brighton BN1 9PX, U.K.

[∥]Medicines Discovery Institute, Cardiff University, Park Place, Cardiff CF10 3AT, U.K.

Supporting Information

ABSTRACT: Aminoglycosides (AGs) are broad-spectrum antibiotics used for the treatment of serious bacterial infections but have use-limiting side effects including irreversible hearing loss. Here, we assessed the otoprotective profile of carvedilol in mouse cochlear cultures and in vivo zebrafish assays and investigated its mechanism of protection which, we found, may be mediated by a block of the hair cell's mechanoelectrical transducer (MET) channel, the major entry route for the AGs. To understand the full otoprotective potential of carvedilol, a series of 18 analogues were prepared and evaluated for their effect against AG-induced damage as well as their affinity for the MET channel. One derivative was found to confer greater protection than carvedilol itself in cochlear cultures and also to bind more tightly to the MET channel. At higher concentrations, both carvedilol and this derivative were toxic in cochlear cultures but not in zebrafish, suggesting a good therapeutic window under in vivo conditions.

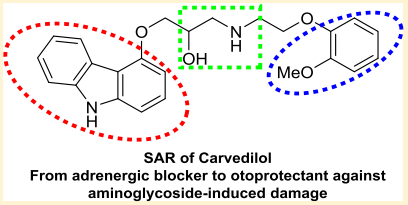

SAR of Carvedilol
From adrenergic blocker to otoprotectant against aminoglycoside-induced damage

INTRODUCTION

Aminoglycosides (AGs) are broad-spectrum antibiotics widely prescribed to treat severe bacterial infections.[1−3] Despite being highly efficacious, they cause unfortunate side effects such as reversible nephrotoxicity and irreversible hearing loss, with the latter occurring in up to 25% of treated patients.[4] The AGs can enter the sensory hair cells of the inner ear through both endocytic processes[5] and specialized cation channels, the mechanoelectrical transducer (MET) channels that are located at the tips of the stereocilia and are responsible for the detection of sounds and body movements.[6−9] The mechanism of ototoxicity is not fully understood and it differs amongst the various AGs, with neomycin and gentamicin, for instance, being shown to activate different cell-death pathways once inside zebrafish lateral line hair cells.[10−12] Once inside the cell, they are thought to interact with various targets such as ribosomes, the endoplasmic reticulum, and mitochondria,[13,14] leading to the production of cytotoxic levels of reactive oxygen species (ROS) which, in turn, cause apoptosis.[15] It is this AG-induced hair cell death that underlies the hearing loss associated with clinical drug treatments. Aside from the redesign of novel AGs[16,17] or hair cell regeneration approaches,[18] methods aimed at preventing this use-limiting side effect have primarily focused on either preventing the entry of AGs into hair cells by identifying blockers of the MET channel[14] or by reducing the cellular accumulation of ROS, often by application of antioxidants, in an attempt to prevent the induction of apoptosis.[14,19] Recent efforts in this field have led to the identification of otoprotective agents able to reduce or prevent the AG-induced hearing loss both in in vitro[20−23] and in in vivo models of AG ototoxicity.[24]

Here, we investigated the otoprotective potential of carvedilol, an FDA-approved nonselective α1- and β-adrenergic blocker (Figure 1), used clinically for the treatment of hypertension, angina, and symptomatic chronic heart failure. Carvedilol has previously been reported to protect against

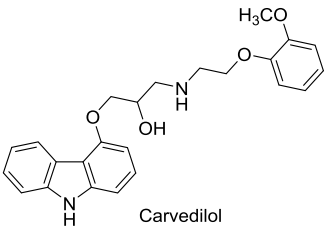

Carvedilol

Figure 1. Structure of carvedilol, a nonselective α1- and β-adrenergic blocker.

Received: August 22, 2018
Published: May 14, 2019

neomycin damage in lateral line hair cells of zebrafish when tested at 10 μM against 200 μM neomycin.[22] In addition, carvedilol did not abrogate the antimicrobial properties of neomycin, making any interference with the bactericidal activity of AGs unlikely[22] and making it an ideal chemical starting point for further investigation.

In this study, we report its protective properties against gentamicin-induced hair cell damage in mouse cochlear cultures. We propose the mechanism by which it offers otoprotection with data supporting the block of the MET channel as being responsible for its otoprotective effect. We synthesized and evaluated a series of novel carvedilol derivatives aimed at improving the protective efficacy and affinity for the MET channel, whilst concurrently reducing toxicity.

RESULTS

Carvedilol Protects Mammalian Sensory Hair Cells from Gentamicin Damage. Mouse cochlear cultures were used to assess whether carvedilol can protect mammalian hair cells from the death induced by exposure to 5 μM gentamicin for 48 h. A concentration of 5 μM gentamicin is optimal, as it is close to the estimated concentration of 1 μM gentamicin reached in the endolymph in vivo at the onset of ototoxic symptoms,[25] and it kills >90% of the basal cells while sparing the apical cells, consistent with the predominantly high-frequency hearing loss observed in patients treated with AGs.[4] On an average, incubation with 5 μM gentamicin caused a loss of 86% of outer hair cells (OHCs) from the mid-basal region of the cochlea, with 110 ± 2.2 (n = 26) OHCs present in a 300 μm long segment of the control and only 15 ± 2.2 (n = 26) in the gentamicin-treated culture (p < 0.001) (Figure 2A,B).

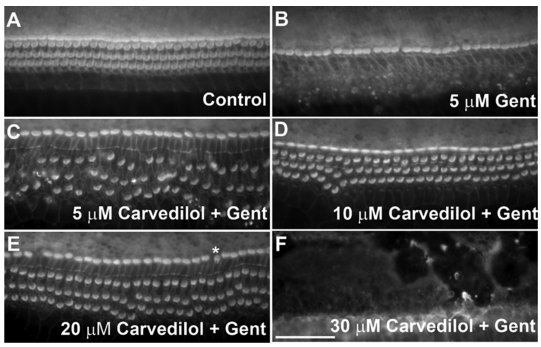

Figure 2. Protective effect of carvedilol against gentamicin-induced damage in a mouse cochlear culture assay. Control cultures exposed to either 0.5% DMSO (A) or 5 μM gentamicin + 0.5% DMSO (B) for 48 h. When coincubated with 5 μM gentamicin, carvedilol was found to be partially protective at 5 μM (C), fully protective at 10 and 20 μM (D,E respectively), and generally cytotoxic at ≥30 μM (F). The asterisk in (E) indicates an example of IHC hair bundle disruption. Scale bar is 50 μm.

Subsequently, mouse cochlear cultures were coincubated with 5 μM gentamicin together with escalating concentrations of carvedilol with the aim to identify the minimal concentration required to provide full protection. When tested at 5 μM, carvedilol provided partial protection, with OHC survival differing significantly from that in both the control and gentamicin-only treated cultures (p < 0.001 in both cases), suggesting that this concentration is at the limit of its protective efficacy (Figure 2C). When tested at 10 and 20 μM, carvedilol provided complete protection against the gentamicin-induced loss of OHCs (p < 0.001) (Figure 2D,E, respectively). Higher concentrations of carvedilol (≥30 μM) proved to be generally cytotoxic, with widespread cell death observed (Figure 2F).

When carvedilol was tested alone, no OHC death was observed at either 10 or 20 μM, with hair cell numbers similar to those observed in controls (Figure 3A–D). Some degree of

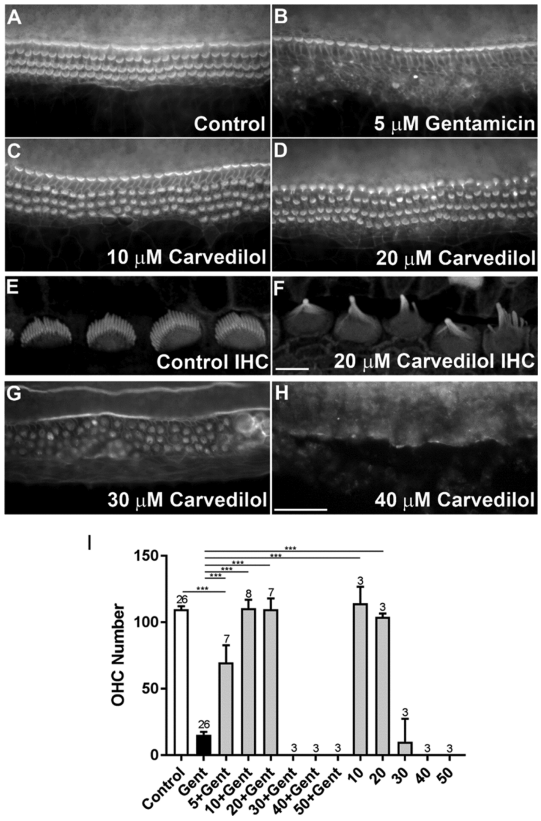

Figure 3. Carvedilol disrupts mechanosensory hair bundles at 20 μM and is generally cytotoxic in vitro at ≥30 μM. Cochlear cultures were exposed for 48 h to 0.5% DMSO (A,E), 5 μM gentamicin + 0.5% DMSO (B), and escalating concentrations of carvedilol: 10 (C), 20 (D,F), 30 (G), and 40 μM (H). Scale bar is 10 (F) and 50 μm (H). Quantification of hair cell survival in a 300 μm long segment of the mid-basal region of cochlear cultures is reported in (I).

inner hair cell (IHC) damage and disruption to hair bundle morphology in both IHCs and OHCs can be observed when tested at 20 μM both alone and in combination with 5 μM gentamicin (Figures 2E and 3D). Figure 3E,F shows confocal images of IHC stereociliary bundles in control conditions (Figure 3E) and after exposure to 20 μM carvedilol (Figure 3F), revealing the full extent of morphological disruption caused by carvedilol.

At concentrations ≥ 30 μM, carvedilol is generally cytotoxic to all cell types in cochlear cultures, both alone and in the presence of 5 μM gentamicin (Figures 2F and 3G,H). Figure 3I summarizes the quantification of OHC survival through analysis of the mid-basal region of cochlear cultures for both carvedilol alone and also coexposed with gentamicin.

Carvedilol Exerts Its Otoprotective Effect by Acting as a Permeant Blocker of the Hair Cell's MET Channel. Despite a narrow therapeutic window in vitro, we decided to investigate the potential mechanism by which carvedilol

DOI: 10.1021/acs.jmedchem.8b01325
J. Med. Chem. 2019, 62, 5312−5329

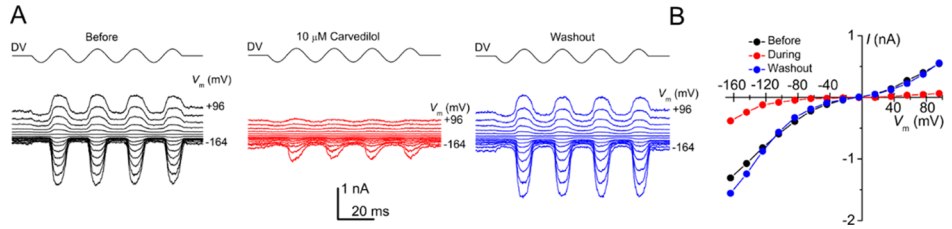

Figure 4. Extracellular exposure to carvedilol reduces OHC MET currents at all potentials, with the reduction most pronounced at intermediate and depolarized potentials. (A) MET currents recorded from a basal-coil OHC between −164 and +96 mV before, during, and after exposure to 10 μM carvedilol. (B) Current−voltage relationships of the currents shown in A reveal the current block at all potentials during carvedilol exposure and the reversibility of the block following washout. The capacitance of the cell was 7.4 pF.

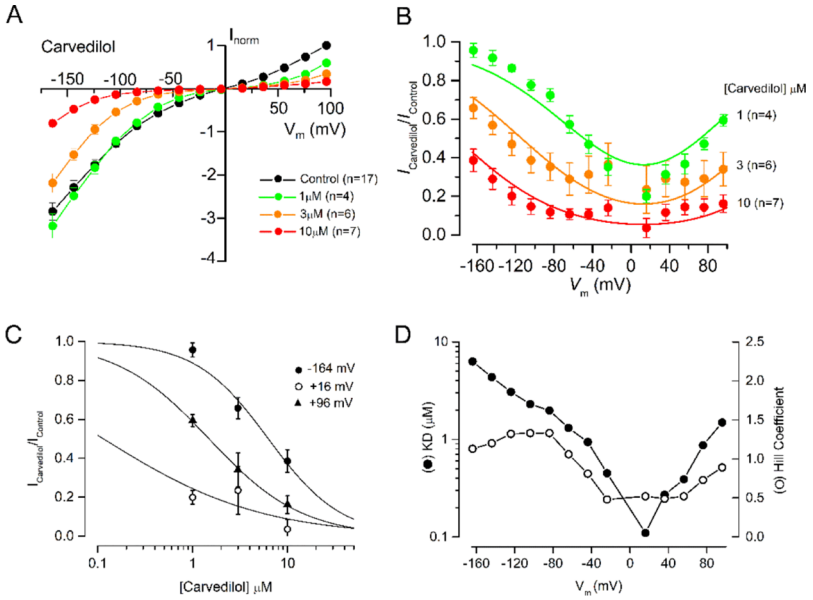

Figure 5. Carvedilol acts as a relatively high-affinity permeant blocker of the MET channel. (A) Average normalized current−voltage relationships for the peak MET currents recorded before and during exposure to 1, 3, and 10 μM carvedilol with currents normalized to the peak control current measured at +96 mV for each cell. (B) Fractional block curves of the current during carvedilol exposure (1, 3, and 10 μM) relative to the control current at each membrane potential. Data are fitted with two barrier−one binding site model (see the Experimental Section). Parameters for the fits are ΔE (the difference in free energy between the intracellular and extracellular barrier) $-0.63kT$; E_b (the free energy of the binding site) $-15.4kT$; δ_b (the electrical distance of the binding site from the extracellular side) 0.53; z (the electrical charge of the blocker) 1.0; Hill coefficient 1.0. Maximum block occurs at +12.8 mV. (C) Dose−response curves derived from the currents recorded at −164, +16, and +96 mV and fit with eq 1. −164 mV: K_D 6.3 μM, Hill coefficient 1.1; +16 mV: K_D 0.1 μM, Hill coefficient 0.5; +96 mV: K_D 1.5 μM, Hill coefficient 0.9. (D) Values of the half-blocking concentration and Hill coefficient at each membrane potential.

provides its protective effect. It is well established that AGs can enter hair cells via their MET channels[7,9] and that block of this channel reduces or prevents their entry into the cells, thereby protecting them from any toxicity resulting from intracellular accumulation. To determine whether carvedilol protects via an interaction with the MET channel, we recorded MET currents from OHCs both before and during extracellular superfusion of carvedilol at concentrations of 1, 3, and 10 μM.

Figure 4A shows an example of the MET currents recorded before (black), during (red), and after (blue) exposure to carvedilol (10 μM), at membrane potentials ranging from −164 to +96 mV. Carvedilol reduces the size of MET currents at all membrane potentials, with this reduction particularly pronounced at intermediate and depolarized potentials. Upon re-exposure to the control solution, the currents recover, indicating a reversible block of the channel. The voltage-dependent block and subsequent recovery of the currents can also be clearly seen from the current−voltage relationships as shown in Figure 4B.

Average normalized current−voltage relationships derived from all cells recorded from at the three different concentrations tested, normalized to the maximum control current at +96 mV for each cell, demonstrated both the increase in the block with increasing compound concentration and the voltage-dependence of the block, with the strongest block observed at the intermediate and depolarized potentials (Figure 5A).

Some recovery of the currents can be seen at the extreme depolarized potentials (+96 mV), with even more pronounced recovery at the extreme hyperpolarized potentials (−164 mV). This recovery with hyperpolarization is more evident from the average fractional block curves showing the current during carvedilol superfusion relative to the control current at each membrane potential (Figure 5B). The maximum block is seen at the intermediate membrane potentials for each concentration of carvedilol with some recovery at depolarized potentials and even greater recovery at the extreme hyperpolarized potentials. This recovery at the hyperpolarized potentials is indicative of a permeant blocker with the

DOI: 10.1021/acs.jmedchem.8b01325
J. Med. Chem. 2019, 62, 5312−5329

Scheme 1[a]

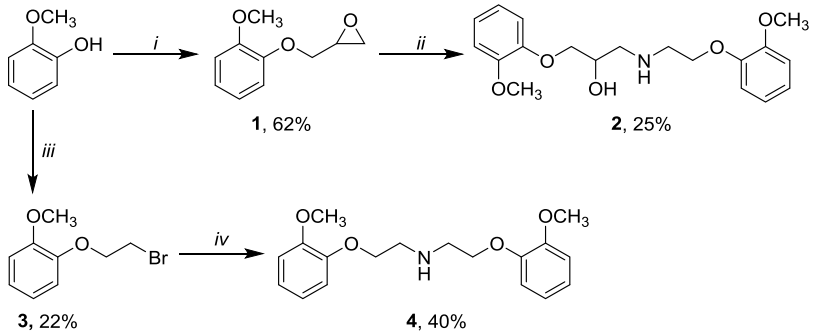

[a]Reagents and conditions: (i) 2-(bromomethyl)oxirane, anhydrous K_2CO_3, DMF, 70 °C, 6 h; (ii) 2-(2-methoxyphenoxy)ethanamine, ethylene glycol dimethyl ether, 80 °C, 6 h; (iii) 1,2-dibromoethane, NaOH, water, reflux, 3 h; (iv) 2-(2-methoxyphenoxy)ethanamine, TEA, THF, 65 °C, 6 h.

Scheme 2[a]

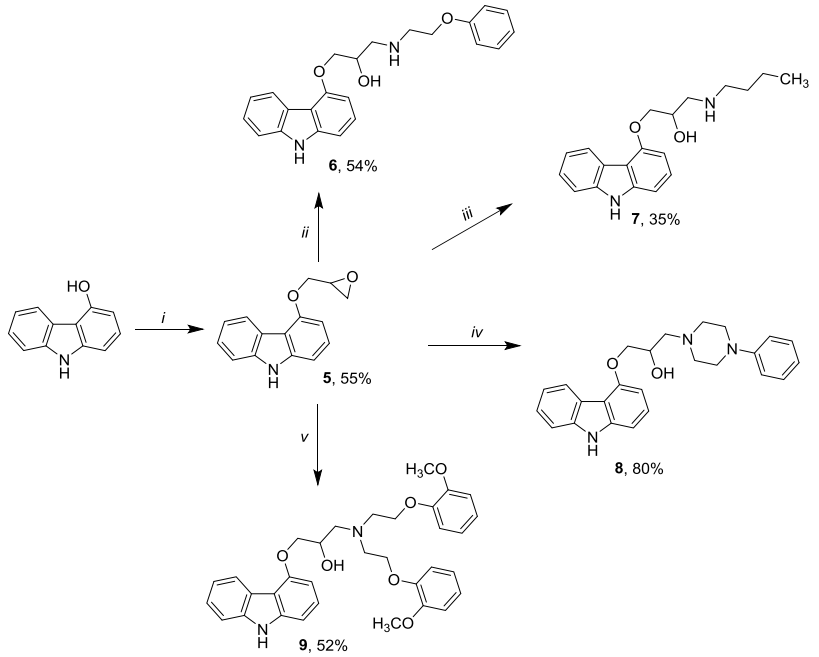

[a]Reagents and conditions: (i) 2-(bromomethyl)oxirane, NaOH, water, DMSO, 45 °C, 16 h; (ii) 2-phenoxyethanamine, ethylene glycol dimethyl ether, 80 °C, 24 h; (iii) butan-1-amine, ethylene glycol dimethyl ether, 80 °C, sealed tube, 24 h; (iv) phenylpiperazine, ethanol, 65 °C, 16 h; (v) **4**, ethylene glycol dimethyl ether, 80 °C, sealed tube, 48 h.

compound, positively charged at physiological pH (calculated pK_a = 8.7), being drawn into the cell by the electrical driving force and therefore reducing the block of the channel. Curves are fitted to a two barrier−one binding site model of the MET channel permeation pathway. Dose−response curves for the extracellular block of the MET channels by carvedilol were generated at each membrane potential and fitted with eq 1 described in the Experimental Section. The dose−response curves derived from the currents at −164, +16, and +96 mV are shown in Figure 5C. The K_D values range from 6.3 μM at −164 mV to 0.1 μM at +16 mV, close to the potential at which the block was strongest (+12.8 mV). The K_D at −84 mV was 2.0 μM, lower than that previously reported for the AG dihydrostreptomycin (DHS), which was found to have a K_D of 7.0 μM at −84 mV in 1.3 mM extracellular Ca^{2+},[7] indicating that carvedilol is a relatively high affinity blocker of the MET channel. Figure 5D reports the K_D and Hill coefficient values for each dose−response curve showing the strongest interaction near +16 mV. The Hill coefficients ranged from 0.5 to 1.3, suggesting that two molecules may interact with the channel, potentially showing negative cooperativity.[26]

These results demonstrate that carvedilol is a relatively high-affinity permeant blocker of the MET channel and consistently protects OHCs from AGs damage at 10 and 20 μM. However, in vitro, it appears to be cytotoxic at higher concentrations.

Chemistry. Driven by these results, we decided to investigate the potential of carvedilol as the chemical starting point for future drug development. We aimed at enhancing its protective effect in mouse cochlear cultures, increasing its block of the MET channel current and reducing the cytotoxicity observed in vitro. We decided to investigate its structure by modifying the carbazole moiety, the anisole ring, and the β-hydroxyl amino group. We first synthesized compound **2** by substituting the carbazole with anisole. The

DOI: 10.1021/acs.jmedchem.8b01325
J. Med. Chem. 2019, 62, 5312−5329

Scheme 3[a]

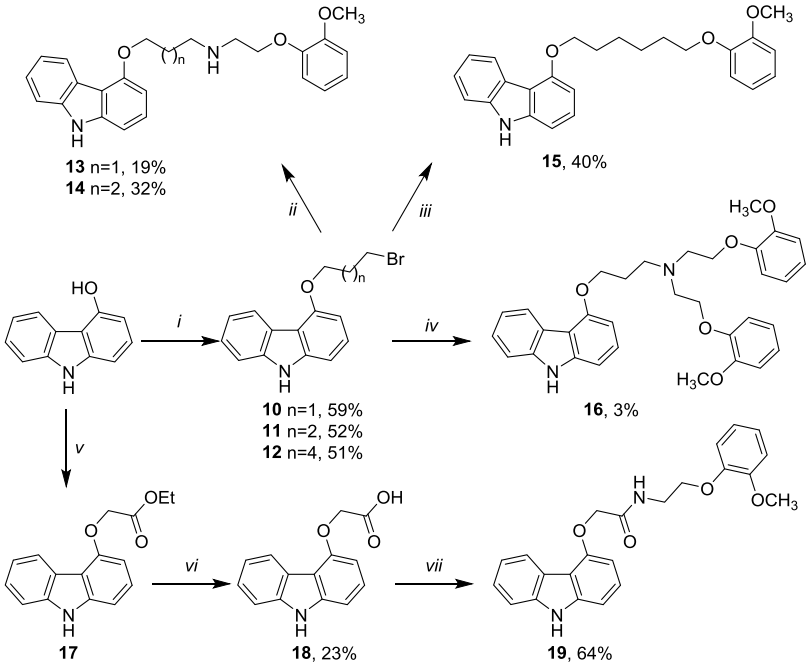

[a]Reagents and conditions: (i) 1,3-dibromopropane for **10**, 1,4-dibromobutane for **11**, 1,6-dibromohexane for **12**, KOH, acetonitrile, rt, 5-18 h; (ii) 2-(2-methoxyphenoxy)ethanamine, anhydrous K_2CO_3, DMF, rt, 16 h for **13**; 2-(2-methoxyphenoxy)ethanamine, TEA, THF, 65 °C, 24 h for **14**; (iii) 2-methoxyphenol, KOH, acetonitrile, rt, 66 h; (iv) **4**, K_2CO_3, DMF, rt, 36 h; (v) ethyl chloroacetate, K_2CO_3, acetone, reflux, 16 h; (vi) 1 N aqueous NaOH, THF, rt, 16 h; (vii) 2-(2-methoxyphenoxy)ethanamine, HOBt, EDC·HCl, DIPEA, DMF, rt, 16 h.

Scheme 4[a]

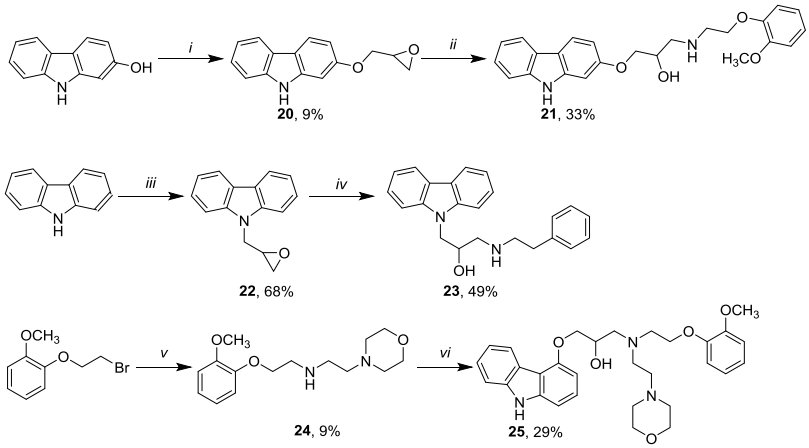

[a]Reagents and conditions: (i) 2-(bromomethyl)oxirane, sodium hydroxide, water, DMSO, 45 °C, 16 h; (ii) 2-(2-methoxyphenoxy)ethanamine, ethanol, 65 °C, 16 h; (iii) 2-(bromomethyl)oxirane, potassium hydroxide, acetonitrile, rt, 20 h; (iv) 2-phenylethylamine, ethanol, 65 °C, 16 h; (v) 4-(2-aminoethyl)morpholine, TEA, THF, 65 °C, 4 h; (vi) 4-(oxiran-2-ylmethoxy)-9*H*-carbazole, ethanol, 65 °C, 16 h.

synthesis involved the preparation of **1** by coupling 2-methoxyphenol and 2-(bromomethyl)oxirane followed by epoxide ring opening with commercially available 2-(2-methoxyphenoxy)ethanamine in ethylene glycol dimethyl ether at 80 °C, providing the desired compound in moderate yield (Scheme 1).

In parallel, to simplify the structure of carvedilol and likely removing its interactions with adrenergic receptors, we investigated the requirement for the *β*-hydroxyl amino group by evaluating compound **4**, which was prepared by coupling 2-(2-methoxyphenoxy)ethanamine and **3**, which was previously made by reacting 2-methoxyphenol with 1,2-dibromoethane.

We then investigated the role of the anisole ring by simplifying to a simple phenol **6** and an aliphatic chain **7**; the role of the basic center by inserting a cyclic tertiary amine (phenyl-piperazinyl) **8** and a tertiary amine bearing two 2-(2-methoxyphenoxy)ethanamine moieties **9**. These compounds are prepared starting from the common intermediate **5**, which is prepared by reacting 4-hydroxycarbazole with 2-(bromomethyl)oxirane in good yield. The epoxide ring is then opened by the appropriate amine using ethylene glycol dimethyl ether as solvent for **6**, **7**, and **9** in moderate to good yield, while in the case of **8**, ethanol was used as solvent, affording the desired compound in 80% yield (Scheme 2).

DOI: 10.1021/acs.jmedchem.8b01325
J. Med. Chem. 2019, 62, 5312−5329

We then investigated the role of the hydroxyl group by preparation of **13**, the carbazole-amine linker **14**, removing the β-hydroxyl amine by linking the carbazole and the anisole rings via a six carbon chain **15** and removing the basic center by the introduction of an amidic bond **19**. Based on the biological data obtained with compounds **9** and **13**, we combined these modifications to make compound **16**. For the synthesis, 4-hydroxycarbazole was reacted with either 1,3-dibromopropane, 1,4-dibromobutane, or 1,6-dibromohexane to give compounds **10**−**12**, respectively. Compounds **10** and **11** were coupled with 2-(2-methoxyphenoxy)ethanamine, yielding **13** and **14**, while compound **12** was coupled with 2-methoxyphenol to give **15** in moderate yield. Compound **16** was obtained by coupling **10** with **4**. For the preparation of the amide analogue **19**, 4-hydroxycarbazole was reacted with ethyl chloroacetate to afford ester **17**, which was hydrolyzed with aqueous sodium hydroxide providing acid **18**. Coupling with 2-(2-methoxyphenoxy)ethanamine was performed under standard amide coupling conditions using 1-hydroxybenzotriazole (HOBt) and *N*-(3-dimethylaminopropyl)-*N*′-ethylcarbodiimide (EDC) affording the desired compound **19** in good yield (Scheme 3).

We then investigated two isomers of carvedilol: 2-hydroxycarvedilol derivative **21**, which was obtained by opening the epoxide ring of compound **20** with 2-(2-methoxyphenoxy)ethanamine, providing the desired compound **21** in moderate yield (Scheme 4); and the 1-carbazole isomer by directly linking the side chain to the nitrogen of the carbazole ring. First, carbazole reacted with epichlorohydrin to yield compound **22** followed by epoxide ring opening using 2-phenylethylamine, obtaining compound **23** in 49% yield.

Finally, to improve the solubility of compound **9**, we designed compound **25** in which one of the 2-methoxyphenoxy group was substituted with a morpholine ring. Compound **3** was reacted with commercially available 4-(2-aminoethyl)-morpholine to obtain compound **24** which was then coupled with **5** to give the desired compound **25** in 29% yield.

Carvedilol Derivatives: Protective Abilities and MET Channel Block. The newly synthesized compounds were screened to assess their protective ability against 5 μM gentamicin using mouse cochlear cultures initially at 20 μM, a concentration at which carvedilol provided full protection and was not cytotoxic. Any compounds that showed full or partial protection were then screened at lower concentrations to establish their minimal protective concentration. We initially designed and synthesized 6 compounds aimed at evaluating the chemical moiety essential for the interaction with the MET channel, and these include modification at the carbazole (**2** and **4**) and anisole (**6** and **7**) rings, the removal of the hydroxyl group (**13**), and the introduction of a second 2-phenoxyethyl moiety to form a tertiary amine (**9**). When tested at 20 μM (Figure 6), compounds **2** and **4** lacking the carbazole moiety provided no protection (Figure 6C,D), while compound **6** with a phenyl group instead of the anisole proved to be generally cytotoxic (Figure 6E). Compound **9**, bearing two 2-methoxyphenoxyethyl moieties, offered only partial protection (Figure 6G), while compounds **7** and **13** consistently protected against OHC loss (Figure 6F,H). As a reference, control cochlear cultures exposed to 0.5% dimethyl sulfoxide (DMSO, Figure 6A) and 5 μM gentamicin (Figure 6B) as well as quantification for both controls and cultures exposed to compounds (Figure 6I) are included.

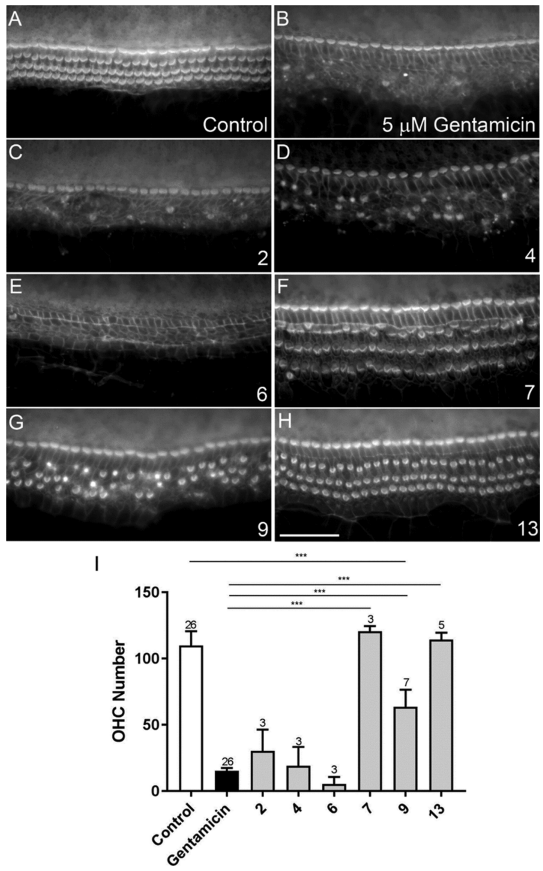

Figure 6. Otoprotective effect of compounds **2**, **4**, **6**, **7**, **9**, and **13** in cochlear cultures against 5 μM gentamicin. (A) Control culture exposed to 0.5% DMSO for 48 h. (B) Culture exposed to 5 μM gentamicin + 0.5% DMSO for 48 h. (C−H) Cultures exposed to 5 μM gentamicin for 48 h + 20 μM: (C) **2**, (D) **4**, (E) **6**, (F) 7, (G) **9**, and (H) **13**. Scale bar is 50 μm. (I) Quantification of OHC survival for the control and compound exposed cultures.

The three derivatives (**7**, **9**, and **13**) that showed partial or full protection at 20 μM were subsequently tested at 10 and 5 μM against 5 μM gentamicin. Only compound **13** provided full protection at 5 μM (as well as at 10 μM), showing an improvement compared to the parent compound carvedilol which was only partially protective at 5 μM (Figure 7A−E). As stated before, in the control condition, some 110 OHCs were present in each cochlear segment, reducing to 15 OHCs following exposure to 5 μM gentamicin. Additional exposure to 5 μM carvedilol increased the average number of surviving OHCs to 66 (54% protection), whereas 5 μM compound **13** resulted in 99 surviving OHCs (88% protection) (Figure 7E).

When tested alone, **13** showed similar toxicity characteristics to carvedilol, proving toxic to OHCs at concentrations $\geq$ 30 μM and affecting the IHC and OHC bundle morphology at 20 μM. Contrary to carvedilol, **13** was not toxic at 30 μM when tested together with 5 μM gentamicin, but it did also affect the IHC and OHC bundle morphology (data not shown).

In conjunction with assessing the protective abilities of these six compounds, potential interactions with the MET channel were investigated by recording MET currents from OHCs before and during exposure to 10 μM of each compound. Figure 8 shows the fractional block of the currents during compound exposure relative to the control currents at each membrane potential, revealing that two compounds **4**

DOI: 10.1021/acs.jmedchem.8b01325
J. Med. Chem. 2019, 62, 5312−5329

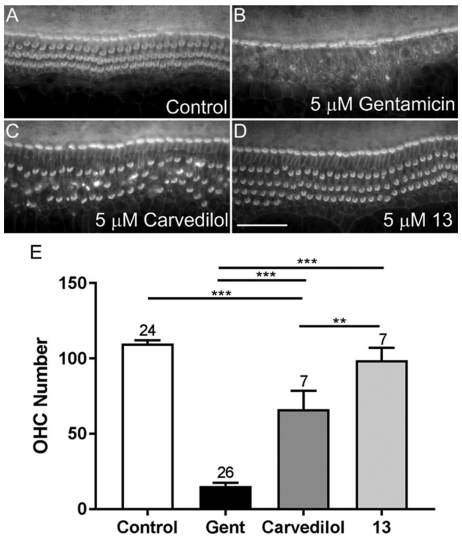

Figure 7. When tested at 5 μM against 5 μM gentamicin, compound **13** showed a greater otoprotective effect. (A) Control culture exposed to 0.5% DMSO for 48 h. (B) Culture exposed to 5 μM gentamicin + 0.5% DMSO for 48 h. (C,D) Cultures exposed to 5 μM gentamicin for 48 h + 5 μM: (C) carvedilol or (D) compound **13**. Scale bar is 50 μm. (E) Quantification of OHC survival for the control and compound-exposed cultures.

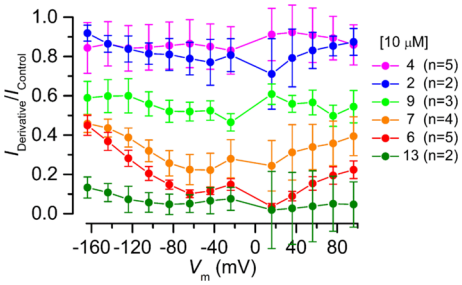

Figure 8. Compounds **2**, **4**, **6**, **7**, **9**, and **13** show varying degrees of inhibition of the MET currents. Fractional block plots of the currents recorded during exposure to 10 μM of each derivative relative to the control currents at each membrane potential.

(magenta) and **2** (blue) have limited interaction with the channel at this concentration.

The poor interaction of compounds **2** and **4** with the MET channel corresponded to the lack of protection observed for these compounds at 20 μM, providing further evidence that the protection offered by carvedilol may come through a block of the MET channel. In addition, these results indicate the need for the carbazole moiety to allow the interaction with the channel. Compound **9** (bright green), which offered only a partial protection at 20 μM, showed approximately 40% block of the MET current at all membrane potentials with no release at extreme hyperpolarized potentials, suggesting this compound may act as a non-permeant blocker. Compounds **6** (red) and **7** (orange) were strong MET channel blockers at 10 μM with a blocking profile similar to carvedilol giving approximately 50−60% block of the current at −164 mV, the most relevant physiological potential. Interestingly, compound **13** (dark green) was the most effective MET channel blocker of this series, providing almost 100% block of the MET current at all membrane potentials. This result is also in accordance with its protective effect, as **13** showed protection of the OHCs from gentamicin damage at concentrations down to 5 μM. This result again suggests that the protection observed is due to a block of the MET channels, reducing the entry of gentamicin into the cells. Compounds **6**, **7**, and **13** appear to be permeant blockers of the MET channel, indicated by the release of the block at the extreme hyperpolarized potentials, and in the case of compound **13**, the release of the block was less pronounced than with carvedilol itself.

A further seven compounds (**8**, **14**, **15**, **19**, **21**, **23**, and **25**) were then designed and synthesized in an attempt to improve protective abilities and physicochemical properties. Of these, **14**, **15**, **21**, and **23** were generally cytotoxic when tested at 20 μM against 5 μM gentamicin (Figure 9D,E,H,I, respectively),

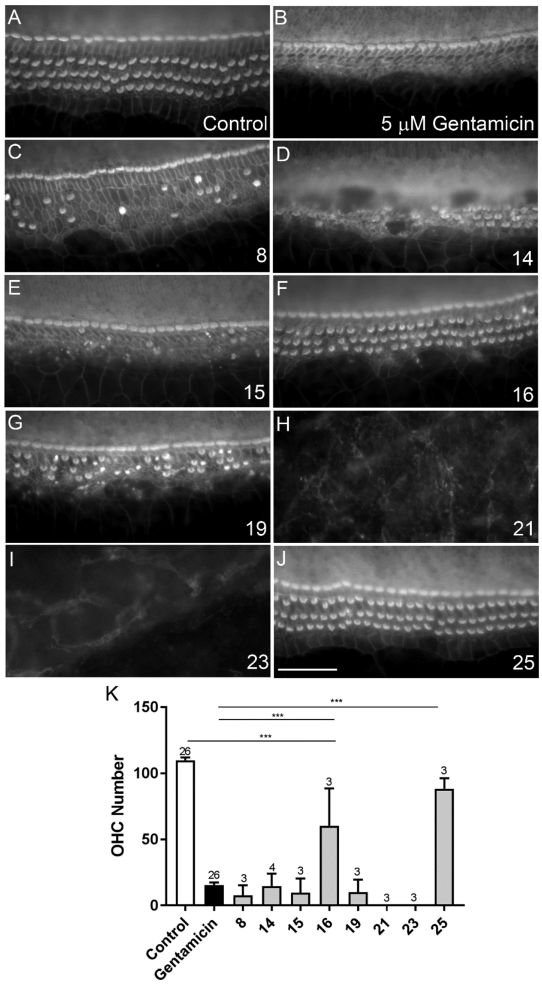

Figure 9. Otoprotective effect of compounds **8**, **14**, **15**, **16**, **19**, **21**, **23**, and **25** in cochlear cultures against 5 μM gentamicin. (A) Control culture exposed to 0.5% DMSO for 48 h. (B) Culture exposed to 5 μM gentamicin + 0.5% DMSO for 48 h. (C−J) Cultures exposed to 5 μM gentamicin for 48 h + 20 μM: (C) **8**, (D) **14**, (E) **15**, (F) **16**, (G) **19**, (H) **21**, (I) **23**, and (J) **25**. Scale bar is 50 μm. (K) Quantification of hair cell survival for the control and cultures exposed to compounds.

19 and **8** offered no protection (Figure 9C,G, respectively), and **25** was consistently protective (Figure 9J). When tested at 10 μM, **25** was protective in 2 out of 4 screens but offered no protection at 5 μM (data not shown). MET channel interactions were subsequently investigated for derivative **25** that showed protection at 20 μM and partial protection at 10

DOI: 10.1021/acs.jmedchem.8b01325
J. Med. Chem. 2019, 62, 5312−5329

μM. The resulting fractional block plot reveals that at a concentration of 10 μM, **25** blocks the MET channel at all membrane potentials (Figure 10). However, the degree of the block is far less than that observed for carvedilol and **13** suggesting this derivative has a reduced affinity for the channel.

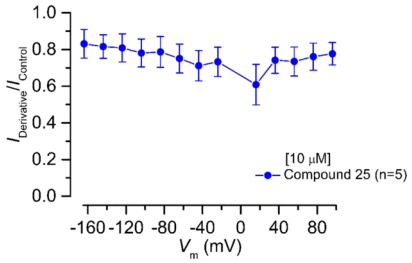

Figure 10. Fractional block plot for compound **25** (10 μM). The size of the current during exposure to the compound relative to the control current at each membrane potential reveals that compound **25** has a low affinity for the MET channel.

Combining the desired characteristics of a nonpermeant MET channel blocker (**9**) with a high-affinity blocker (**13**), we designed, synthesized, and tested a further derivative (**16**). This compound was found fully protective at 20 μM against 5 μM gentamicin on only one out of three occasions (Figure 9F), with no protection in the other two trials. The lack of consistency with the data was probably caused by the poor solubility of the compound. When tested at 10 μM, compound **16** did not offer any protection (data not shown). When tested in our electrophysiology assay, compound **16** showed limited interaction with the MET channel at both 3 and 10 μM (data not shown).

Assessing the Protective Effect and MET Channel Properties of Adrenergic Receptor and Calcium Channel Blockers. We then proceeded to investigate whether the adrenergic (α and β) receptors, primary pharmacological targets of carvedilol, play a role in its otoprotective abilities. We tested the nonselective β-blocker propranolol **26**, the selective β_1-blocker CGP20712 **27**, the selective α_1-blocker naftopidil **28**, and the nonselective adrenergic blocker and calcium channel-blocker verapamil **29** (Figure 11).

Compounds **26**, **27**, and **29** did not offer any protection against 5 μM gentamicin when tested at 20 μM (Figure 12C,D,F, respectively), while **28** proved to be partially effective under the same conditions (Figure 12E,G). However, when the test concentration was lowered to 10 μM, compound **28** did not protect cochlear culture hair cells against gentamicin damage (data not shown).

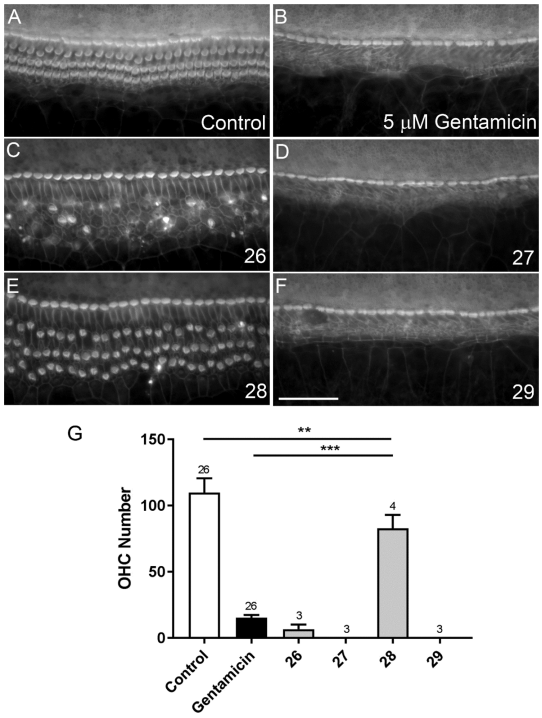

Figure 12. Otoprotective effect of compounds **26**, **27**, **28**, and **29** in cochlear cultures against 5 μM gentamicin. (A) Control culture exposed to 0.5% DMSO for 48 h. (B) Culture exposed to 5 μM gentamicin + 0.5% DMSO for 48 h. (C–F) Cultures exposed to 5 μM gentamicin for 48 h + 20 μM: (C) **26**, (D) **27**, (E) **28**, and (F) **29**. (G) Quantification of hair cell survival for the control and compound exposed cultures. Scale bar is 50 μm.

We subsequently investigated the affinity of the partially protective compound **28** for the MET channel. This compound did not interact strongly with the MET channel which is revealed from the fractional block plot shown in Figure 13.

Electrophysiological Properties of Compound 13: A Strong Permeant MET Channel Blocker. The cochlear culture protection assay revealed that carvedilol derivative **13**, at a concentration of 5 μM, displayed a consistent protective effect against 5 μM gentamicin. When tested on its own,

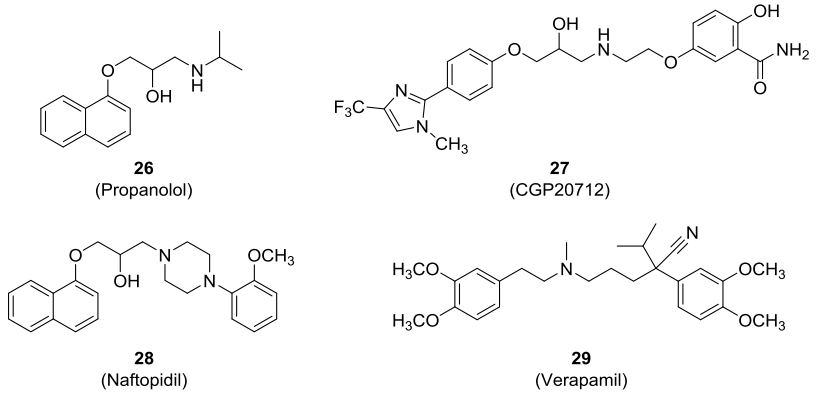

Figure 11. Chemical structures of other adrenergic blockers (**26**–**28**) and calcium channel-blocker **29** used in this study.

DOI: 10.1021/acs.jmedchem.8b01325
J. Med. Chem. 2019, 62, 5312–5329

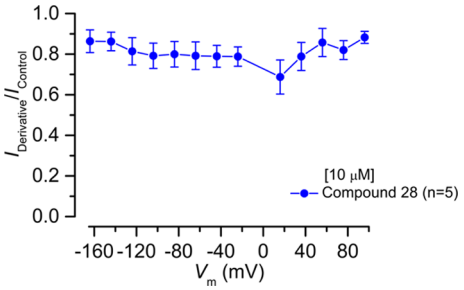

Figure 13. Fractional block plot for compound **28**. The size of the current during exposure to the compound relative to the control current at each membrane potential reveals that compound **28** has a low affinity for the MET channel.

compound **13** appears to be cytotoxic at 30 μM. However, when tested in the presence of 5 μM gentamicin, compound **13** is not toxic, suggesting a competitive interaction at the level of the MET channel that may effectively reduce the cytotoxic effects of both compounds. In order to compare MET channel interactions between compound **13** and carvedilol, MET currents were recorded before and during **13** exposure at 1, 3, and 10 μM and the resulting current−voltage relationships, fractional block curves, and dose−response curves generated (Figure 14).

From the average normalized current−voltage relationships (Figure 14A) and the fitted average fractional block curves (Figure 14B) it can be seen that the block of the channel by **13** is very similar to that of carvedilol, with the maximum block seen at the intermediate potentials and release of the block at extreme depolarized and hyperpolarized potentials, indicating that this compound is also a permeant blocker of the MET channel. Dose−response curves were generated, derived from the currents at each membrane potential, and fitted with eq 1 (see Experimental Section). Figure 14C shows the curves derived from the currents at −164, +16, and +96 mV, where the K_D values were found to be 4.6, 1.0, and 1.7 μM, respectively. The K_D at −84 mV (2.4 μM) is similar to that of carvedilol (2.0 μM), suggesting that both compounds are relatively high affinity blockers of the MET channel at a potential close to the resting potential in vitro. The Hill coefficients ranged from 1.1 to 2.0, suggesting there may be two or more binding sites within the channel for **13** (Figure 14D).[26]

Kinetics of MET Channel Block for Carvedilol and Compound 13. One further property of the MET channel interaction that was investigated for both carvedilol and **13** was the kinetics of the block, to determine whether or not these compounds are open-channel blockers, similar to berbamine and D-tubocurarine,[20] or can reside in the closed channel, similar to the permeant MET channel blocker FM1-43.[6] The time course of the block is revealed by applying large force steps to the hair bundles both before and during exposure to the compound and recording the resulting currents. Such currents can be seen before and during exposure to carvedilol (1 and 3 μM; Figure 15A,B) and **13** (1 and 3 μM; Figure 15C,D). From a holding potential of −84 mV, channel opening results in rapidly activating inward currents in all conditions. During the step, the currents show minimal adaptation in control conditions and an exponential decline during both carvedilol and **13** exposure. This suggests that both compounds are open-channel blockers, accessing their binding site once the channel has opened. Time constants were measured from the current decline and found to be 18.0 ± 5.0 ms (1 μM carvedilol; n = 3); 9.6 ± 0.4 ms (3 μM carvedilol; n = 4); 9.9 ± 0.9 ms (1 μM **13**; n = 3); and 6.0 ± 1.6 ms (3 μM **13**; n = 3).

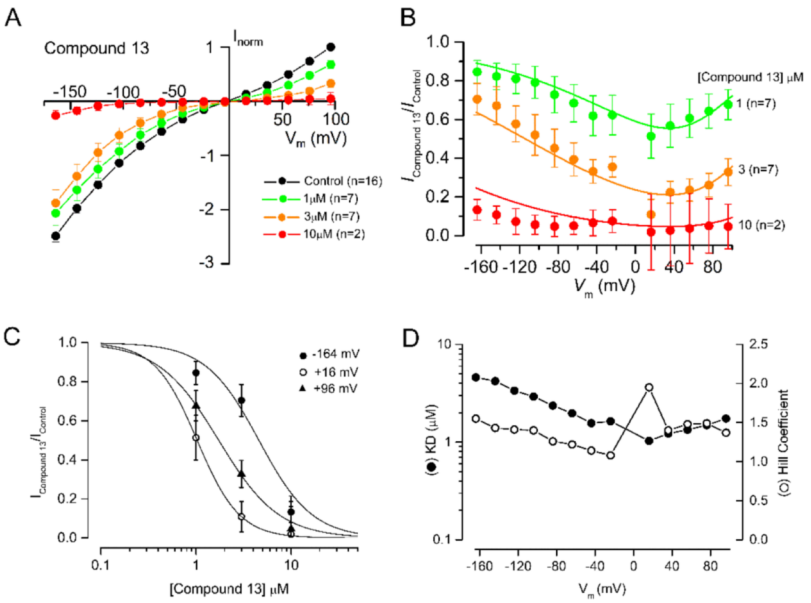

Figure 14. Compound **13** acts as a permeant blocker of the MET channel, with similar blocking properties to carvedilol. (A) Average normalized current−voltage relationships for the peak MET currents recorded before and during exposure to 1, 3, and 10 μM **13**. (B) Fractional block curves for compound **13** tested at 1, 3, and 10 μM reveal that it is a permeant MET channel blocker. Fitting parameters are ΔE −2.22kT; E_b −21.3kT; δ_b 0.71; z 1.0; δ_b 0.71; Hill coefficient 1.4. Maximum block occurs at +33.9 mV. (C) Dose−response curves derived from the currents recorded at −164, +16, and +96 mV and fit with eq 1. −164 mV: K_D 4.6 μM, Hill coefficient 1.6; +16 mV: K_D 1.0 μM, Hill coefficient 2.0; +96 mV: K_D 1.7 μM, Hill coefficient 1.4. (D) Half-blocking concentration and Hill coefficient as a function of membrane potential.

DOI: 10.1021/acs.jmedchem.8b01325
J. Med. Chem. 2019, 62, 5312−5329

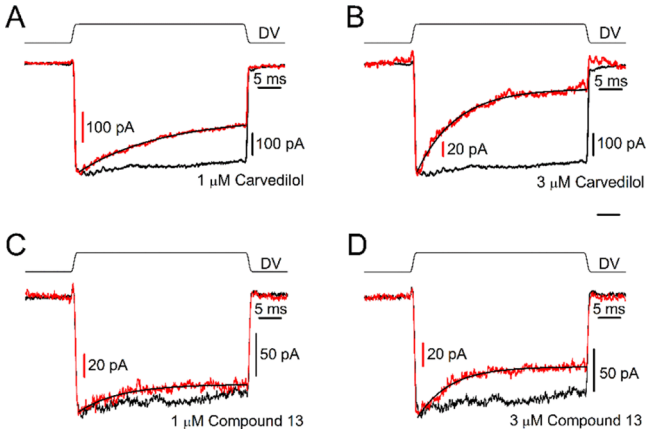

Figure 15. Kinetics of MET channel block mediated by carvedilol and **13** reveals that both act as open-channel blockers. (A–D) Currents resulting from a mechanical step delivered by the fluid jet (±40 V driver voltage, DV shown above each trace), from a holding potential of −84 mV, before (black trace) and during (red trace) superfusion of (A) 1 μM carvedilol, (B) 3 μM carvedilol, (C) 1 μM **13**, and (D) 3 μM **13**. Currents (averaged from 10 repetitions) before and during compound exposure have been scaled and superimposed. The currents during compound superfusion were fitted with single exponentials (A) τ = 19.3 ms, (B) τ = 8.6 ms, (C) τ = 10.1 ms, and (D) τ = 6.9 ms.

From these time constants, entry rates of the drug molecules into the hair cells were calculated (see the Experimental Section), and their energy profiles for permeation through the MET channel pore were determined (Figure 16). Both compounds bind much stronger (free energy $E_b < -15kT$) to the binding site in the channel pore than DHS (E_b $-8.27kT$ at 1.3 mM extracellular Ca^{2+})[7] and the drugs D-tubocurarine ($-8.67kT$) and berbamine ($-12.0kT$) that we evaluated

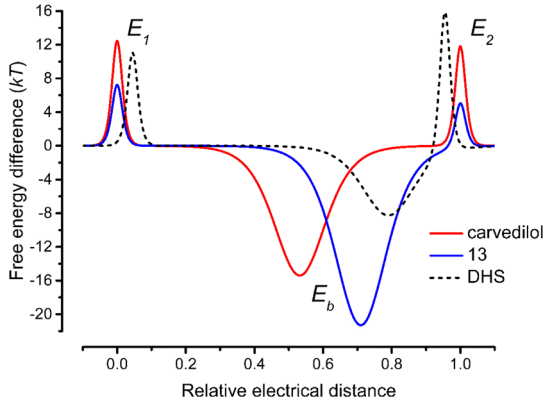

Figure 16. Energy profiles for MET channel permeation and block by carvedilol and **13**. Energy profiles calculated from fits to the fractional block curves and kinetics of MET current block are shown. Values for the free energies of the binding site E_b and barriers E_1 and E_2 are shown in the absence of a voltage across the membrane (V_m = 0 mV). The voltage-independent extracellular barrier E_1, at an electrical distance of zero, has a free energy of $12.5kT$ for carvedilol and $7.23kT$ for **13**. The free energy of E_b is $-15.4kT$ for carvedilol and $-21.3kT$ for **13**. The binding sites, δ_b, are located at an electrical distance from the extracellular side of 0.53 for carvedilol and 0.71 for **13**. The intracellular barrier E_2, positioned at an electrical distance of one, is $11.8kT$ for carvedilol and $5.01kT$ for **13**. For comparison, the energy profile calculated before for DHS in 1.3 mM extracellular Ca^{2+} is shown (dotted line).[7]

before.[20] A consequence of this is that, unlike the other compounds, the maximum block for these monovalent cations (at physiological pH) occurs at positive membrane potentials (Figures 5B and 14B). Moreover, their permeation through the MET channels is considerably slower than DHS. For example, with 1 μM of compound, 80 MET channels with an open probability of 0.1 and a membrane potential of −150 mV, the entry rates into the OHCs are 165 molecules/s for carvedilol and 125 molecules/s for **13**, compared with some 1130 molecules/s for DHS.[7,20] For higher concentrations, the entry rates started to saturate, so they never approach those for DHS (e.g., for 100 μM, rates were 1078 molecules/s for carvedilol, 998 molecules/s for **13**, and 11 460 molecules/s for DHS).

Carvedilol and Compound 13 Reduce GTTR Loading into Hair Cells. To further assess whether carvedilol and **13** protect sensory hair cells against AG damage by preventing the entry of the antibiotics into cells, a fluorescent gentamicin analogue (gentamicin Texas Red: GTTR) was used to enable quantification of gentamicin uptake.[27] Pre-incubation with either 1% DMSO, 100 μM carvedilol or 100 μM **13** for 5 min prior to 0.2 μM GTTR application resulted in significantly reduced loading of GTTR in the presence of both carvedilol and **13** relative to the DMSO control ($p < 0.001$ in both cases) (Figure 17). A significant difference was not observed between the GTTR loading in the presence of carvedilol or **13**. These findings further suggest that both carvedilol and **13** protect against AG damage by competitively blocking the MET channel and thereby preventing AG entry into hair cells, minimizing accumulation and consequent apoptosis induction.

Comparison of Protection and Toxicity of Carvedilol with Compound 13 in Zebrafish Larvae. In order to compare the protective effect of **13** to that of carvedilol in vivo, 4 days post fertilization (dpf) zebrafish larvae were treated with either neomycin or gentamicin in the presence of each compound, and the number of remaining hair cells was assessed (Figure S1A–D). Dose–response curves for carvedilol and compound **13** were constructed, and EC_{50}s (the effective concentration at which 50% of hair cells survive) were derived. The EC_{50}s for carvedilol and **13** protection against neomycin damage were 2.47 and 2.08 μM, respectively. The EC_{50} for carvedilol protection against gentamicin damage was 10.95 μM, whilst for compound **13**, it was 10.81 μM. The protective effect of these compounds therefore extends to other AGs in addition to gentamicin.

We then assessed the toxicity of carvedilol and compound **13** by treating 3 dpf zebrafish larvae with each at 30 and 100 μM for 48 h (see the Supporting Information Methods). At a concentration of 100 μM, carvedilol killed the larvae in two out of three trials, whilst it was not toxic at 30 μM. With compound **13**, neither concentration was toxic for the larvae. Larvae treated with 100 μM carvedilol had slowed or no circulation, while those treated with 30 μM of carvedilol or either concentration of compound **13** had no obvious defects in circulation. Treated larvae were startled and assayed for movement. As expected, larvae treated with 100 μM carvedilol showed reduced movement, whilst those treated with 100 μM of compound **13** showed increased movement compared to the control.

Assessing Effects of Carvedilol and Compound 13 on the Antimicrobial Efficacy of Gentamicin. Carvedilol and compound **13** were tested in a bacterial cell viability assay to identify if either of these compounds decreased the antimicrobial activity of gentamicin. The minimum inhibitory

DOI: 10.1021/acs.jmedchem.8b01325
J. Med. Chem. 2019, 62, 5312–5329

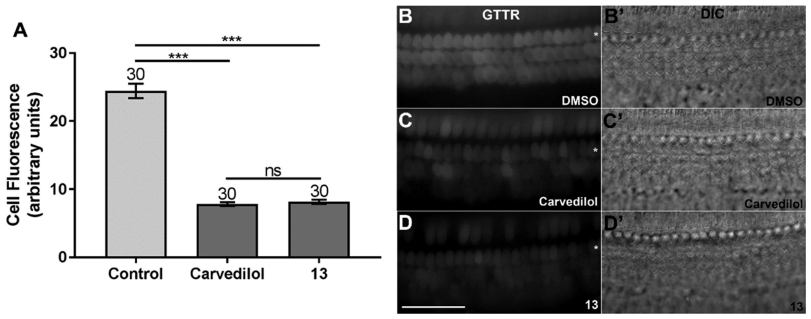

Figure 17. Carvedilol and **13** reduce the entry of GTTR into mouse cochlear culture hair cells. (A) Quantification of GTTR fluorescence intensity in a control culture pretreated with 1% DMSO before the addition of 0.2 μM GTTR, compared to cultures pretreated with 100 μM carvedilol or **13**. Both compounds significantly reduced GTTR loading ($p < 0.001$). No significant difference in reduction was seen between the two compounds. (B–D) Representative fluorescence image from which intensity values were measured and a DIC image for (B,B′) the control (C,C′) carvedilol and (D,D′) **13**. Asterisks indicate the first row of OHCs, from which fluorescence intensity values were taken. $N = 30$ cells, with 10 cells analyzed from three separate experiments. Scale bar is 50 μm.

concentration (MIC) of gentamicin was established for three clinically important bacteria: *Klebsiella pneumoniae*, *Pseudomonas aeruginosa*, and *Staphylococcus aureus*. The bacteria were treated with gentamicin at 1× MIC (2.2 μM) together with 2.2 or 11 μM carvedilol or compound **13** (1× or 5× the gentamicin MIC). Neither of the compounds resulted in an observable reduction in gentamicin antimicrobial activity (Figure S2A–C).

DISCUSSION AND CONCLUSIONS

The nonselective α- and β-adrenergic blocker carvedilol was reported to provide protection against AG damage in a whole zebrafish larval model study.[22] Here, we investigated its potential using a mammalian system of AG-induced toxicity, mouse cochlear cultures, and zebrafish larvae. In parallel, we investigated its potential molecular target by studying its electrophysiological profile. First, we determined that carvedilol (10 and 20 μM) was able to fully protect cochlear cultures against the damage caused by exposure to 5 μM gentamicin for 48 h. Unfortunately, carvedilol proved to be cytotoxic at higher concentrations (≥30 μM) and caused severe damage to the mechanosensory hair bundles when tested at 20 μM, both alone and together with gentamicin. Despite this, we decided to investigate further the mode of protection of carvedilol by studying its potential interaction with the MET channel, which is the main entry route of AGs into hair cells. From our experiments, carvedilol proved to be a relatively high-affinity, permeant, and reversible blocker of the MET current with a K_D of 6.3 μM at a physiologically relevant potential of −164 mV. To fully evaluate its otoprotective profile, we decided to investigate the structure–activity relationship (SAR) of carvedilol, aiming to improve its affinity for the MET channel and its protective effect as well as reducing its cytotoxicity.

From an initial investigation, we established that the carbazole moiety is needed for both protection and interaction with the channel, with neither compound **2** nor **4** protecting hair cells from gentamicin or blocking the MET current. Interestingly, the replacement of the anisole moiety with a phenyl group as in compound **6** led to an increased cytotoxicity while still providing the same level of block of the MET current as its parent derivative carvedilol. The replacement of the anisole for an alkyl chain as in compound **7** led to a retention of its protective effect and only slightly reduced its effect on the MET current. We then investigated the role of the β-amino alcohol linker with regard to its interaction with the channel. The removal of the hydroxyl group, compound **13**, resulted in an almost complete block of the MET current at 10 μM and at least the same protective effect against gentamicin damage compared to carvedilol. These data show that the hydroxyl group is not needed for the interaction with the channel, and we can postulate that the enhanced block of the channel may be derived by an increased basicity of the nitrogen, with a calculated pK_a for compound **13** and carvedilol being 9.3 and 8.7, respectively, which may lead to a stronger interaction with the channel. To our surprise, the extension of just one extra carbon in the alkyl chain spacer between the carbazole and the basic center, compound **14**, proved to be detrimental as the compound was found to be more toxic than the parent compound. The role of the basic center was investigated by substituting the nitrogen with a carbon (**15**) or by making the nitrogen nonbasic (**19**). Neither of these compounds had any protective effect, supporting the need for a basic center that is positively charged at physiological pH for the protective effect. Also unsuccessful was the conversion of the secondary amine into a tertiary cyclic amine, as compound **8** did not have any protective effect against gentamicin damage. In compound **9**, we inserted a second ethyl-anisole moiety, and it was found to interact tightly with the channel and to act as a nonpermeant blocker as noted by the lack of the release of the block at the extreme hyperpolarized (−164 mV) potential, probably due to some new interactions between the channel and the second anisole moiety. However, the level of the block of the MET current was reduced if compared to carvedilol, and it was only partially protective.

We then investigated two isomers of carvedilol moving the side chain to the 2-position (**21**) or linking it to the nitrogen in the carbazole ring (**23**); both compounds were found to be toxic to the cochlear cultures. Driven by the results obtained with compounds **13** (improved protective effect and block of the MET current) and **9** (nonpermeant MET channel blocker), we designed compound **16**, which lacks the hydroxyl group as in compound **13** and has the second ethyl-anisole as in compound **9**. Compound **16** proved to be only partially protective, but we noticed a lack of consistency during the assays which is probably due to the poor solubility of this compound in the biological media, preventing any meaningful interpretation of the results. Whilst we solved the solubility issue for this compound by substituting the second ethyl-

DOI: 10.1021/acs.jmedchem.8b01325
J. Med. Chem. 2019, 62, 5312–5329

anisole moiety with an ethyl morpholine **25**, this did not translate into an increased protective effect. We then investigated other adrenergic and calcium blockers, with compounds **26**, **27**, and **29** (propranolol, CGP20712, and verapamil, respectively) not showing any protective effect, and **28** (naftopidil) only offering partial protection at 20 μM. Interestingly, **28** is the only compound that showed some protection but it does not have the carbazole moiety and bears a naphthol ring. Based on our previous findings showing D-tubocurarine as a potent blocker of the MET channel current (K_D = 2.2 μM) without showing any toxicity at a higher concentration (50 μM),[20] the cytotoxic effect observed with some of these compounds is unlikely to be related to their ability to block the MET channel and is probably series related. A hit-to-lead optimization campaign will be focused on increasing the protective effect, reducing the toxicity, and addressing any adrenergic effect of these compounds. In addition, there will be the possibility of formulating the potential otoprotective agent to allow administration into the inner ear via transtympanic injection.

From a mechanistic point of view, we investigated in more detail the interaction of **13**, the most protective derivative, with the MET channel. This compound showed a very similar interaction with the channel to carvedilol, having a K_D of 4.6 μM at a potential of −164 mV. Kinetics of the MET channel block showed that both carvedilol and **13** are open-channel blockers, suggesting that they are able to interact with the channel only when it is open. As shown in the energy profiles graph, both carvedilol and **13** bind tighter to the negatively charged vestibule of the MET channel compared to the AG DHS with a longer time consequently spent inside the channel. This result reflects on the rate of entry into the cells for these compounds, which is considerably lower (10 fold) compared to DHS. This stronger interaction with the MET channel may be behind the protective effect offered by carvedilol and **13** which hinders the interaction of AG with the channel and as a consequence reducing its entry into the hair cells. The stronger protection of **13** (E_b −21.3kT) compared to carvedilol may be due to its binding inside the channel pore more strongly than carvedilol (E_b −15.4kT) (Figure 16). Both carvedilol and compound **13** were able to block the loading of GTTR into the hair cells, further supporting the notion that the protective effect of both compounds is due to their block of the MET channel and the prevention of AG uptake into hair cells.

Finally, to exclude a protective effect specific to gentamicin, we compared the protection of carvedilol and compound **13** against neomycin using hair cells in the lateral line organs of zebrafish larvae. Both compounds were protective against neomycin damage at a concentration of ≥12.5 μM, and found to be slightly less effective when tested against gentamicin, providing full protection at a concentration ≥ 25 μM. In addition, neither carvedilol nor compound **13** interfered with gentamicin antimicrobial activity.

In conclusion, we established that carvedilol is able to protect cochlear cultures from AG-induced damage, although it is also cytotoxic in vitro at higher concentrations. We have established a clear SAR identifying the need for a carbazole moiety, a basic center, and preferentially an anisole moiety. The toxicity observed in vitro with cochlear cultures may not be an issue as carvedilol is widely used in the clinic and is not associated with hearing loss. Furthermore, carvedilol and its derivatives did not show a toxic effect in vivo with zebrafish larvae at 30 μM. Although the "therapeutic window" is narrow in vitro, our current data show that carvedilol and its derivatives are a valid chemical starting point for the future development of drugs that will prevent AGs induced ototoxicity, and that the MET channel is a potential target for such compounds.

EXPERIMENTAL SECTION

All commercial reagents were purchased from Sigma-Aldrich, Alfa Aesar, Apollo Scientific, Fluorochem or Tokyo Chemical Industry and of the highest available purity. Unless otherwise stated, chemicals were used as supplied without further purification. Anhydrous solvents were purchased from Acros (AcroSeal) or Sigma-Aldrich (SureSeal) and were stored under nitrogen. Petroleum ether refers to the fraction with a boiling point between 40 and 60 °C. Thin-layer chromatography: precoated aluminum-backed plates (60 F254, 0.2 mm thickness, Merck) were visualized under both short- and long-wave UV light (254 and 366 nm). Flash column chromatography was carried out using commercial prepacked columns from Biotage, Isco, Grace, or filled with Merck silica gel 60 (40−63 μm) or C18 silica on an ISCO Combiflash Rf or a Biotage Isolera Prime. HPLC purification was performed on an Agilent 1100 series HPLC spectrometer, using a Phenomenex Luna 10 μm C18 150 mm × 15 mm column, eluted using water and acetonitrile at 15 mL/min and detected at 254 nm.

Proton nuclear magnetic resonance spectra were recorded at 500 or 600 MHz on a Varian VNMRS 500 MHz or Varian VNMRS 600 MHz spectrometers, respectively (at 30 °C), using residual isotopic solvent ($CHCl_3$, δ = 7.27 ppm, DMSO δ = 2.50 ppm) as an internal reference. Chemical shifts are quoted in parts per million (ppm). Coupling constants (J) are recorded in hertz (Hz). The following abbreviations are used in the assignment of NMR signals: s (singlet), d (doublet), t (triplet), q (quartet), qn (quintet), m (multiplet), bs (broad singlet), dd (doublet of doublet), and dt (doublet of triplet). Carbon nuclear magnetic resonance spectra were recorded at 125 or 151 MHz on Varian 500 or 600 MHz spectrometers, respectively, and are proton-decoupled, using residual isotopic solvent ($CHCl_3$, δ = 77.00 ppm, DMSO δ = 39.52 ppm) as an internal reference.

LCMS data were recorded on a Waters 2695 HPLC using a Waters 2487 UV detector and a Thermo LCQ ESI-MS. Samples were eluted through a Phenomenex Lunar 3 μm C18 50 mm × 4.6 mm column, using water and acetonitrile acidified by 0.1% formic acid at 1 mL/min and detected at 254 nm. The following methods were used: method 1: water (+0.1% formic acid)/acetonitrile (+0.1% formic acid) = from 65/35 to 10/90 in 3.5 min, then isocratic 10/90 0.4 min, then from 10/90 to 65/35 in 0.1 min; method 2: water (+0.1% formic acid)/acetonitrile (+0.1% formic acid) = from 70/30 to 10/90 in 5 min, then isocratic 10/90 1.0 min, then from 10/90 to 70/30 in 0.5 min, and then isocratic 70/30 for 0.5 min.

LCMS (MDAP): LCMS data were recorded on a Shimatzu Prominence Series coupled to a LCMS-2020 ESI and APCI mass spectrometer. Samples were eluted through a Phenomenex Gemini 5μ C18 110A 250 mm × 4.6 mm column, using water and acetonitrile acidified by 0.1% formic acid at 1 mL/min and detected at 254 nm. The following method, marked as method 3, was used: water (+0.1% formic acid)/acetonitrile (+0.1% formic acid) = isocratic 95/5 1 min, then from 95/5 to 5/95 in 20 min, then isocratic 5/95 for 4 min, and then from 5/95 to 70/30 in 5 min.

Physicochemical properties were calculated using MarvinSketch 16.8.15.0 by ChemAxon (https://www.chemaxon.com).

Compound purity was assured by a combination of high-field multinuclear NMR (H, C) and HPLC; purity by the later was always >95%.

Chemistry. *Synthesis of 2-((2-Methoxyphenoxy)methyl)oxirane (**1**).* A mixture of 2-methoxyphenol (1.0 g, 8.06 mmol), 2-(bromomethyl)oxirane (0.69 mL, 8.06 mmol), and anhydrous K_2CO_3 (2.23 g, 16.11 mmol) in dimethylformamide (DMF, 5 mL) was stirred at 70 °C for 6 h. After cooling, the solvent was evaporated under reduced pressure, the residue was dissolved in water, and the aqueous phase was extracted with ethyl acetate. The organic phase

DOI: 10.1021/acs.jmedchem.8b01325
J. Med. Chem. 2019, 62, 5312−5329

was washed with saturated $NaHCO_3$ solution, dried over $MgSO_4$, filtered, and concentrated. The residue was then purified by flash column chromatography gradient elution of petroleum ether/ethyl acetate (100/0 to 0/100) to give **1** as an oil which crystallized to give a colorless solid (0.90 g, 62%). ^{1}H NMR (DMSO 600 MHz): δ 6.95 (td, J = 7.6, 1.6 Hz, 2H), 6.90 (td, J = 7.7, 1.6 Hz, 1H), 6.85 (td, J = 7.6, 1.6 Hz, 1H), 4.25 (dd, J = 11.3, 2.8 Hz, 1H), 3.78 (dd, J = 11.3, 6.6 Hz, 1H), 3.74 (s, 3H), 3.30 (d, J = 2.6 Hz, 1H), 2.81 (dd, J = 5.1, 4.2 Hz, 1H), 2.67 (dd, J = 5.1, 2.7 Hz, 1H).

*Synthesis of 1-(2-Methoxyphenoxy)-3-[2-(2-methoxyphenoxy)-ethylamino]propan-2-ol (**2**).* A solution of 2-(2-methoxyphenoxy)-ethanamine (0.84 mL, 5.55 mmol) in ethylene glycol dimethyl ether (1 mL) was heated to 80 °C. Then, a solution of **1** (0.25 g, 1.39 mmol) in ethylene glycol dimethyl ether (1 mL) was added dropwise, and the reaction mixture was stirred at 80 °C for 5 h. Then, **1** (0.12 g, 0.67 mmol) in ethylene glycol dimethyl ether (0.50 mL) was added dropwise, and the reaction mixture was stirred at 80 °C for further 1 h. After cooling, the solvent was evaporated under reduced pressure, and the residue was purified by flash column chromatography gradient elution of petroleum ether/ethyl acetate (100/0 to 0/100). The compound was further purified by HPLC gradient elution of water/acetonitrile = 95:5 to 0:100 in 20 min to give **2** as a colorless solid (0.12 g, 25%). ^{1}H NMR (DMSO 500 MHz): δ 6.96−6.94 (m, 4H), 6.89−6.85 (m, 4H), 4.95 (s, 1H), 3.99 (t, J = 5.6 Hz, 2H), 3.93−3.83 (m, 3H), 3.73 (d, J = 3.2 Hz, 6H), 2.88 (t, J = 5.6 Hz, 2H), 2.80−2.71 (m, 1H), 2.68−2.60 (m, 1H). ^{13}C NMR (DMSO 126 MHz): δ 149.78, 149.71, 148.83, 148.66, 121.55, 121.45, 121.25, 121.23, 114.40, 114.26, 113.01, 112.93, 72.13, 69.08, 68.78, 56.07, 53.03, 48.98. LCMS: method 2: RT: 0.71 min; M + H$^+$: 348.38. LCMS: method 3, RT = 11.22 min; M + H$^+$: 348.40.

*Synthesis of 1-(2-Bromoethoxy)-2-methoxy-benzene (**3**).* A solution of 2-methoxyphenol (4.0 mL, 36.38 mmol) and NaOH (4.37 g, 109.13 mmol) in water (25 mL) was added dropwise to 1,2-dibromoethane (25.08 mL, 291.03 mmol), and the reaction mixture was then stirred at reflux for 3 h. After cooling, the phases were separated, and the organic phase was concentrated. The residue was purified by flash column chromatography gradient elution of petroleum ether/ethyl acetate (100/0 to 50/50) to give a yellow oil which crystallized at room temperature to give **3** as a yellow solid (1.84 g, 22%). ^{1}H NMR (DMSO 500 MHz): δ 7.00−6.95 (m, 2H), 6.95−6.91 (m, 1H), 6.89−6.84 (m, 1H), 4.27 (t, J = 5.5 Hz, 2H), 3.80−3.73 (m, 5H).

*Synthesis of 2-(2-Methoxyphenoxy)-N-[2-(2-methoxyphenoxy)-ethyl]ethanamine (**4**).* 2-(2-Methoxyphenoxy)ethanamine (0.90 mL, 5.98 mmol) and tryethylamine (TEA, 1.67 mL, 11.96 mmol) were added to a solution of **3** (1.38 g, 5.98 mmol) in tetrahydrofuran (THF, 10 mL), and the reaction mixture was stirred at 65 °C for 5 h. Then, TEA (0.83 mL, 5.98 mmol) was added, and the reaction mixture was stirred at 65 °C for further 1 h. After cooling, the solvent was removed under reduced pressure, and the residue was triturated with water and ethyl acetate. The precipitate was filtered to give a first crop of the desired compound as a colorless solid (0.52 g, 26%). The layers were then separated, and the aqueous phase was extracted with ethyl acetate. The combined organic phase was washed with brine, dried over $MgSO_4$, filtered, and concentrated to give **4** as a yellow oil which crystallized at room temperature. The solid was washed four times with a mixture of water/ethyl acetate (5/1) to give a second crop of the desired compound **4** as an off-white solid (0.28 g, 14%). ^{1}H NMR (DMSO 600 MHz): δ 6.96−6.93 (m, 4H), 6.89−6.82 (m, 4H), 4.00 (t, J = 5.6 Hz, 4H), 3.72 (s, 6H), 2.93 (t, J = 5.6 Hz, 4H). ^{13}C NMR (DMSO 151 MHz): δ 149.64, 148.49, 121.52, 121.16, 114.16, 112.66, 68.93, 55.88, 48.67. LCMS: method 2: RT: 0.68 min; M + H$^+$: 318.12. LCMS: method 3, RT = 11.37; M + H$^+$: 318.35.

*Synthesis of 4-(Oxiran-2-ylmethoxy)-9H-carbazole (**5**).* To a solution of NaOH (0.48 g, 12.01 mmol) in water (10 mL), 9*H*-carbazol-4-ol (2.0 g, 10.92 mmol) and DMSO (5 mL) were added followed by dropwise addition of 2-(bromomethyl)oxirane (1.4 mL, 16.37 mmol). The reaction mixture was then heated at 45 °C for 16 h. After cooling, water (20 mL) was added, and the reaction mixture was stirred at room temperature for 1 h. The precipitate formed was filtered, and the wet solid was recrystallized from isopropanol to give **5** as a brown solid (0.82 g, 31%). A second crop of **5** was also obtained as a brown solid (0.63 g, 24%). ^{1}H NMR (DMSO 600 MHz): δ 11.26 (s, 1H), 8.15 (d, J = 7.8 Hz, 1H), 7.44 (d, J = 8.0 Hz, 1H), 7.33 (dt, J = 8.2, 7.1 Hz, 1H), 7.28 (t, J = 8.0 Hz, 1H), 7.17−7.11 (m, 1H), 7.08 (d, J = 8.0 Hz, 1H), 6.68 (d, J = 7.9 Hz, 1H), 4.54 (dd, J = 11.2, 2.6 Hz, 1H), 4.08 (dd, J = 11.2, 6.2 Hz, 1H), 3.52 (ddd, J = 6.5, 4.4, 2.5 Hz, 1H), 2.92 (t, J = 4.7 Hz, 1H), 2.83 (dd, J = 5.1, 2.7 Hz, 1H). ^{13}C NMR (DMSO 151 MHz): δ 154.93, 141.56, 139.39, 126.89, 125.10, 122.72, 122.00, 119.09, 111.93, 110.91, 104.68, 101.14, 69.21, 50.38, 44.26. LCMS: method 2: RT: 3.65 min; M + H$^+$: 240.16.

*Synthesis of 1-(9H-Carbazol-4-yloxy)-3-(2-phenoxyethylamino)-propan-2-ol (**6**).* A solution of 2-phenoxyethanamine (0.22 mL, 1.67 mmol) in ethylene glycol dimethyl ether (0.75 mL) was heated at 80 °C, and then a solution of **5** (0.10 g, 0.42 mmol) in ethylene glycol dimethyl ether (0.75 mL) was added dropwise, and the reaction mixture was stirred at 80 °C for 24 h. After cooling, the solvent was removed under reduced pressure, and the residue was purified by flash column chromatography gradient elution of petroleum ether/ethyl acetate (100/0 to 0/100) to give the desired compound which was further purified by reverse phase HPLC gradient elution of water/acetonitrile = 95:5 to 0:100 in 20 min to give **6** as an off-white solid (0.085 g, 54%). ^{1}H NMR (DMSO 600 MHz): δ 11.21 (s, 1H), 8.20 (d, J = 7.8 Hz, 1H), 7.42 (d, J = 8.0 Hz, 1H), 7.34−7.28 (m, 1H), 7.28−7.21 (m, 3H), 7.10 (t, J = 7.4 Hz, 1H), 7.05 (d, J = 8.0 Hz, 1H), 6.89 (dd, J = 7.9, 6.3 Hz, 3H), 6.66 (d, J = 7.9 Hz, 1H), 5.13 (d, J = 4.9 Hz, 1H), 4.19−4.11 (m, 2H), 4.11−4.06 (m, 1H), 4.01 (t, J = 5.6, 2H), 2.93 (td, J = 5.5, 2H), 2.81 (dd, J = 11.9, 6.8 Hz, 1H), 2.01 (s, 1H). ^{13}C NMR (DMSO 151 MHz): δ 159.02, 155.40, 141.53, 139.34, 129.88, 126.92, 124.94, 122.90, 122.17, 119.00, 114.86, 112.00, 110.77, 104.25, 100.87, 70.89, 68.91, 67.86, 53.08, 48.90. LCMS: method 2: RT: 1.53 min; M + H$^+$: 377.19.

*Synthesis of 1-(Butylamino)-3-(9H-carbazol-4-yloxy)propan-2-ol (**7**).* A solution of butan-1-amine (0.50 mL, 5.02 mmol) in ethylene glycol dimethyl ether (0.75 mL) was heated at 80 °C in a sealed tube. Then, a solution of **5** (0.12 g, 0.50 mmol) in ethylene glycol dimethyl ether (0.75 mL) was added dropwise, and the reaction mixture was stirred at 80 °C for 2.5 h. After cooling, the solvent was removed under reduced pressure, and the residue was left overnight, continuing the reaction with no solvent. The residue was then purified by flash column chromatography gradient elution of petroleum ether/ethyl acetate (100/0 to 0/100) to give the desired compound as a yellow gum, which was further purified by reverse phase HPLC gradient elution of water/acetonitrile = 95/5 to 0/100 in 20 min to give **7** as a pale yellow solid (0.055 g, 35%). ^{1}H NMR (DMSO 500 MHz): δ 11.21 (s, 1H), 8.21 (d, J = 7.7 Hz, 1H), 7.43 (d, J = 8.0 Hz, 1H), 7.35−7.30 (m, 1H), 7.28 (t, J = 8.0 Hz, 1H), 7.12 (t, J = 7.4 Hz, 1H), 7.06 (d, J = 8.0 Hz, 1H), 6.67 (d, J = 7.9 Hz, 1H), 5.04 (br s, 1H), 4.18−4.11 (m, 2H), 4.09−4.04 (m, 1H), 2.83 (dd, J = 11.9, 4.8 Hz, 1H), 2.73 (dd, J = 11.9, 6.8 Hz, 1H), 2.55 (dt, J = 6.9, 2.8 Hz, 2H), 1.47−1.35 (m, 2H), 1.35−1.25 (m, 2H), 0.85 (t, J = 7.3 Hz, 3H). ^{13}C NMR (DMSO 126 MHz): δ 155.47, 141.59, 139.40, 126.90, 124.94, 122.90, 122.23, 118.94, 110.78, 109.99, 104.25, 100.95, 71.05, 68.84, 53.19, 49.61, 32.28, 20.39, 14.36. LCMS: method 2: RT: 0.69 min; M + H$^+$: 313.02. LCMS: method 3, RT = 11.65; M + H$^+$: 313.35.

*Synthesis of 1-(9H-Carbazol-4-yloxy)-3-(4-phenylpiperazin-1-yl)-propan-2-ol (**8**).* A mixture of **5** (0.20 g, 0.84 mmol) and phenyl piperazine (0.13 mL, 0.84 mmol) in ethanol (25 mL) was stirred at 65 °C for 16 h. The reaction solvent was then removed under reduced pressure, and the residue was purified by flash column chromatography gradient elution of petroleum ether/ethyl acetate (100/0 to 0/100) to give **8** as a colorless oil which crystallized on standing (0.28 g, 80%). ^{1}H NMR ($CDCl_3$ 500 MHz): δ 8.29 (d, J = 7.8 Hz, 1H), 8.09 (s, 1H), 7.44−7.37 (m, 1H), 7.37−7.21 (m, 5H), 7.06 (d, J = 8.1 Hz, 1H), 6.95 (d, J = 8.1, 2H), 6.88 (t, J = 7.3 Hz, 1H), 6.69 (d, J = 8.0 Hz, 1H), 4.42−4.29 (m, 2H), 4.28−4.23 (m, 1H), 3.32−3.19 (m, 5H), 2.95−2.87 (m, 1H), 2.87−2.75 (m, 2H), 2.73−2.65 (m, 2H). ^{13}C NMR ($CDCl_3$ 126 MHz): δ 151.17, 150.82, 144.11, 138.69, 129.13, 126.66, 125.01, 122.93, 119.88, 119.67, 117.73, 116.15,

DOI: 10.1021/acs.jmedchem.8b01325
J. Med. Chem. 2019, 62, 5312−5329

110.01, 103.82, 101.21, 70.28, 65.85, 61.07, 53.46, 53.31, 49.30. LCMS: method 3, RT = 12.39; M + H$^+$: 402.25.

*Synthesis of 1-[Bis[2-(2-methoxyphenoxy)ethyl]amino]-3-(9H-carbazol-4-yloxy)propan-2-ol (**9**).* A solution of **4** (0.13 g, 0.42 mmol) in ethylene glycol dimethyl ether (0.50 mL) was heated in a sealed tube at 80 °C. A solution of **5** (0.10 g, 0.42 mmol) in ethylene glycol dimethyl ether (0.50 mL) was added dropwise, and the reaction was heated at 80 °C for 5 h. Then, **4** (0.13 g, 0.42 mmol) was added, and the reaction mixture was stirred at 80 °C for 24 h. Then, a solution of **4** (0.07 g, 0.21 mmol) in ethylene glycol dimethyl ether (0.50 mL) was added, and the reaction mixture was stirred at 80 °C for further 18 h. After cooling, the solvent was removed under reduced pressure, and the residue was purified by flash column chromatography gradient elution of petroleum ether/ethyl acetate (100/0 to 0/100) to give the desired compound which was further purified by flash column chromatography gradient elution of petroleum ether/ethyl acetate (100/0 to 20/100) to give the desired compound as a yellow oil which was triturated with methanol/acetone to give **9** as a colorless solid (0.12 g, 52%). ^{1}H NMR (DMSO 600 MHz): δ 11.20 (s, 1H), 8.22 (d, J = 7.7 Hz, 1H), 7.40 (d, J = 8.1 Hz, 1H), 7.31−7.25 (m, 1H), 7.22 (t, J = 8.0 Hz, 1H), 7.09−7.00 (m, 2H), 6.88 (d, J = 8.0 Hz, 2H), 6.84−6.80 (m, 2H), 6.75−6.69 (m, 4H), 6.58 (d, J = 7.9 Hz, 1H), 4.92 (d, J = 4.6 Hz, 1H), 4.23−4.15 (m, 2H), 4.14−4.07 (m, 1H), 4.00−3.95 (m, 4H), 3.65 (s, 6H), 3.05−2.96 (m, 5H), 2.83 (dd, J = 13.3, 6.0 Hz, 1H). ^{13}C NMR (DMSO 151 MHz): δ 155.47, 149.41, 148.45, 141.53, 139.33, 126.91, 124.88, 122.90, 122.22, 121.17, 121.07, 118.96, 113.45, 112.58, 111.99, 110.73, 104.13, 100.65, 70.37, 68.42, 67.42, 58.54, 55.86, 54.74. LCMS: method 2: RT: 2.37 min; M + H$^+$: 557.40. LCMS: method 3, RT = 14.04 min; M + H$^+$: 557.60.

*Synthesis of 4-(3-Bromopropoxy)-9H-carbazole (**10**).* A solution of 4-hydroxycarbazole (0.50 g, 2.73 mmol), 1,3-dibromopropane (0.83 mL, 8.19 mmol), and KOH (0.15 g, 2.73 mmol) in acetonitrile (25 mL) was stirred at room temperature overnight. After this period, 1,3-dibromopropane (0.42 mL, 4.09 mmol) and KOH (0.046 g, 0.82 mmol) were added, and the stirring was continued for further 3 h. The solvent was then removed under reduced pressure, and the residue was purified by flash column chromatography gradient elution of petroleum ether/ethyl acetate (100/0 to 50/50) to give **10** as a colourless solid (0.50 g, 59%). ^{1}H NMR ($CDCl_3$ 500 MHz): δ 8.25 (d, J = 7.8 Hz, 1H), 8.07 (s, 1H), 7.46−7.37 (m, 2H), 7.36−7.30 (m, 1H), 7.26−7.22 (m, 1H), 7.07 (d, J = 8.1 Hz, 1H), 6.71 (d, J = 8.0 Hz, 1H), 4.41 (t, J = 5.8 Hz, 2H), 3.78 (t, J = 6.5 Hz, 2H), 2.55 (p, J = 6.2 Hz, 2H). LCMS: method 1: RT: 3.67 min; M + H$^+$: 304.06, 306.05.

*Synthesis of 4-(4-Bromobutoxy)-9H-carbazole (**11**).* A mixture of 4-hydroxycarbazole (0.50 g, 2.73 mmol), 1,4-dibromobutane (0.89 mL, 8.19 mmol), and KOH (0.15 g, 2.73 mmol) in acetonitrile (25 mL) was stirred at room temperature for 16 h. The solvent was removed under reduced pressure, and the residue was purified by flash column chromatography gradient elution of petroleum ether/ethyl acetate (100/0 to 50/50) to give **11** as a colorless solid (0.47 g, 52%). ^{1}H NMR ($CDCl_3$ 500 MHz): δ 8.28 (d, J = 7.8 Hz, 1H), 8.05 (s, 1H), 7.43−7.36 (m, 2H), 7.32 (t, J = 8.0 Hz, 1H), 7.27−7.22 (m, 1H), 7.04 (d, J = 8.1 Hz, 1H), 6.66 (d, J = 8.0 Hz, 1H), 4.27 (t, J = 5.8 Hz, 2H), 3.58 (t, J = 6.4 Hz, 2H), 2.27−2.21 (m, 2H), 2.20−2.13 (m, 2H). ^{13}C NMR ($CDCl_3$ 126 MHz): δ 138.65, 137.28, 126.65, 124.93, 122.93, 119.65, 117.73, 109.94, 103.49, 100.97, 88.29, 88.28, 66.76, 33.64, 29.61, 28.00. LCMS: method 1: RT: 3.84 min; M + H$^+$: 318.03, 319.95.

*Synthesis of 4-(6-Bromohexoxy)-9H-carbazole (**12**).* A solution of 4-hydroxy carbazole (0.50 g, 2.73 mmol), 1,6-dibromohexane (1.26 mL, 8.19 mmol), and KOH (0.31 g, 5.46 mmol) in acetonitrile (25 mL) was stirred at room temperature for 5 h. Then, the solvent was removed under reduced pressure, and the residue was purified by flash column chromatography gradient elution of petroleum ether/ethyl acetate (100:0 to 0:100) to give **12** as a pale yellow solid (0.48 g, 51%). ^{1}H NMR (DMSO 600 MHz): 11.21 (s, 1H), 8.13 (dd, J = 7.8, 1.2 Hz, 1H), 7.43 (dt, J = 8.2, 0.9 Hz, 1H), 7.31 (ddd, J = 8.1, 7.1, 1.2 Hz, 1H), 7.26 (t, J = 8.0 Hz, 1H), 7.13 (ddd, J = 7.9, 7.2, 1.0 Hz, 1H), 7.04 (d, J = 8.0 Hz, 1H), 6.65 (d, J = 7.9 Hz, 1H), 4.17 (t, J = 6.3 Hz, 2H), 3.53 (t, J = 6.7 Hz, 2H), 1.91−1.82 (m, 4H), 1.63−1.45 (m, 4H). LCMS: method 2: RT: 6.00 min; M + H$^+$: 346.10, 348.06. Another fraction was isolated to give the bis-alkylated product as a yellow solid (0.20 g, 14%).

*Synthesis of 3-(9H-Carbazol-4-yloxy)-N-[2-(2-methoxyphenoxy)-ethyl]propan-1-amine (**13**).* A solution of **10** (0.10 g, 0.33 mmol), 2-(2-methoxyphenoxy)ethanamine (0.15 mL, 0.99 mmol), and anhydrous K_2CO_3 (0.14 g, 0.99 mmol) in anhydrous DMF (5 mL) was stirred at room temperature under a nitrogen atmosphere overnight. The solvent was then removed under reduced pressure, and the residue was dissolved in DCM. The organic phase was washed with water (five times), dried over $MgSO_4$, filtered, and concentrated. The residue was purified by flash column chromatography gradient elution of petroleum ether/ethyl acetate (100/0 to 0/100). The compound obtained was then further purified by HPLC gradient elution of water/acetonitrile = 95/5 to 0/100 in 20 min to give **13** as an off-white solid (0.025 g, 19%). ^{1}H NMR (DMSO 600 MHz): δ 11.21 (s, 1H), 8.13 (d, J = 7.8 Hz, 1H), 7.42 (d, J = 8.0 Hz, 1H), 7.30 (ddd, J = 8.2, 7.1, 1.2 Hz, 1H), 7.26 (t, J = 8.0 Hz, 1H), 7.14−7.07 (m, 1H), 7.04 (d, J = 8.0 Hz, 1H), 6.93−6.90 (m, 2H), 6.86 (td, J = 7.7, 1.7 Hz, 1H), 6.82 (td, J = 7.6, 1.6 Hz, 1H), 6.67 (d, J = 7.9 Hz, 1H), 4.25 (t, J = 6.1 Hz, 2H), 3.98 (t, J = 5.8 Hz, 2H), 3.70 (s, 3H), 2.93−2.82 (m, 4H), 2.04 (p, J = 6.5 Hz, 2H). ^{13}C NMR (DMSO 151 MHz): δ 155.44, 149.64, 148.51, 141.51, 139.34, 126.94, 124.91, 122.56, 122.20, 121.46, 121.15, 119.03, 114.15, 112.66, 111.89, 110.83, 104.15, 100.85, 68.83, 66.14, 55.88, 48.77, 46.61, 30.04. LCMS: method 2: RT: 1.77 min; M + H$^+$: 391.25; LCMS: method 3, RT = 12.64; M + H$^+$: 391.45.

*Synthesis of 4-(9H-Carbazol-4-yloxy)-N-[2-(2-methoxyphenoxy)-ethyl]butan-1-amine (**14**).* To a solution of **11** (0.25 g, 0.79 mmol) in THF (20 mL) were added TEA (0.24 mL, 1.74 mmol) and 2-(2-methoxyphenoxy)ethanamine (0.13 g, 0.79 mmol), and the reaction was stirred at 65 °C for 4 h. The reaction mixture was cooled to room temperature and 2-(2-methoxyphenoxy)ethanamine (0.13 g, 0.79 mmol) and TEA (0.16 mL, 1.18 mmol) were added. The reaction mixture was reheated to 65 °C and stirred for further 20 h. After cooling, the solvent was removed under reduced pressure, and the residue was purified by flash column chromatography gradient elution of petroleum ether/ethyl acetate (100/0 to 0/100) to give **14** as a colorless oil (0.11 g, 32%). ^{1}H NMR ($CDCl_3$ 500 MHz): δ 8.31 (d, J = 7.6 Hz, 2H), 7.41−7.33 (m, 2H), 7.31 (t, J = 8.0 Hz, 1H), 7.25−7.20 (m, 1H), 7.02 (d, J = 8.1 Hz, 1H), 6.97−6.86 (m, 4H), 6.64 (d, J = 8.0 Hz, 1H), 4.21 (t, J = 6.5 Hz, 2H), 4.14 (t, J = 5.2 Hz, 2H), 3.84 (s, 3H), 3.05 (t, J = 5.3 Hz, 2H), 2.76 (t, J = 7.3 Hz, 2H), 2.10−1.92 (m, 2H), 1.83−1.72 (m, 3H). ^{13}C NMR ($CDCl_3$ 126 MHz): δ 155.60, 140.94, 138.70, 126.63, 124.82, 123.03, 122.72, 121.47, 120.90, 119.54, 114.01, 112.61, 111.79, 109.98, 109.89, 103.31, 100.95, 88.27, 68.77, 67.74, 55.78, 49.56, 48.83, 27.31, 26.82. LCMS: method 3, RT = 12.74; M + H$^+$: 405.20.

*Synthesis of 4-[6-(2-Methoxyphenoxy)hexoxy]-9H-carbazole (**15**).* A solution of **12** (0.10 g, 0.29 mmol), 2-methoxyphenol (0.06 mL, 0.58 mmol), and KOH (0.03 g, 0.58 mmol) in acetonitrile (8 mL) was stirred at room temperature for 6 h. Then, 2-methoxyphenol (0.06 mL, 0.58 mmol) and KOH (0.03 g, 0.58 mmol) were added, and the stirring continued for further 60 h. After this period, the solvent was removed under reduced pressure, and the residue was purified by flash column chromatography gradient elution of petroleum ether/ethyl acetate (100:0 to 60:40) to give the desired compound which was washed with methanol to give **15** as an off-white solid (0.045 g, 40%). ^{1}H NMR (DMSO 600 MHz): δ 11.21 (s, 1H), 8.12 (d, J = 7.8 Hz, 1H), 7.42 (d, J = 8.0 Hz, 1H), 7.32−7.28 (m, 1H), 7.26 (t, J = 8.0 Hz, 1H), 7.09 (t, J = 7.5 Hz, 1H), 7.04 (d, J = 8.0 Hz, 1H), 6.91 (td, J = 7.7, 1.8 Hz, 2H), 6.87−6.80 (m, 2H), 6.66 (d, J = 7.9 Hz, 1H), 4.19 (t, J = 6.3 Hz, 2H), 3.94 (t, J = 6.5 Hz, 2H), 3.71 (s, 3H), 1.92 (p, J = 6.6 Hz, 2H), 1.76 (p, J = 6.8 Hz, 2H), 1.63 (p, J = 7.5 Hz, 2H), 1.55 (q, J = 7.8 Hz, 2H). ^{13}C NMR (DMSO 600 MHz): δ 155.45, 149.54, 148.66, 141.52, 139.34, 126.94, 124.91, 122.52, 122.20, 121.20, 121.16, 119.03, 113.74, 112.69, 111.89,

DOI: 10.1021/acs.jmedchem.8b01325
J. Med. Chem. 2019, 62, 5312−5329

110.83, 104.15, 100.84, 68.53, 67.71, 55.92, 40.24, 29.30, 29.22, 25.94, 25.74. LCMS: method 2: RT: 5.96 min; M + H^+: 390.10.

*Synthesis of 3-(9H-Carbazol-4-yloxy)-N,N-bis[2-(2-methoxyphenoxy)ethyl]propan-1-amine (**16**).* A solution of **4** (0.32 g, 0.97 mmol), **10** (0.10 g, 0.32 mmol), and K_2CO_3 (0.13 g, 0.97 mmol) in anhydrous DMF (5 mL) was stirred at room temperature under a nitrogen atmosphere for 36 h. The solvent was then removed under reduced pressure, and the residue was purified by three sequential flash column chromatography: first column, gradient elution of DCM/methanol = 90/10; second column, gradient elution of DCM/methanol = (100/0 to 99/1); and third column, gradient elution of petroleum ether/ethyl acetate (100/0 to 0/100) to give **16** as a colorless solid (4.8 mg, 3%). ^{1}H NMR ($CDCl_3$ 500 MHz): δ 8.29 (d, J = 7.8 Hz, 1H), 8.07 (s, 1H), 7.47−7.33 (m, 2H), 7.30 (t, J = 8.0 Hz, 1H), 7.18 (t, J = 7.4 Hz, 1H), 7.03 (d, J = 8.1 Hz, 1H), 6.92−6.83 (m, 5H), 6.83−6.73 (m, 4H), 6.65 (d, J = 8.0 Hz, 1H), 4.32 (t, J = 6.0 Hz, 2H), 4.16−4.09 (m, 4H), 3.80 (s, 5H), 3.12 (t, J = 6.4 Hz, 4H), 3.03 (t, J = 6.9 Hz, 2H), 2.20 (p, J = 6.5 Hz, 2H). ^{13}C NMR ($CDCl_3$ 126 MHz): δ 159.00, 155.63, 151.71, 146.04, 136.37, 129.83, 126.69, 124.81, 122.91, 120.96, 120.82, 119.65, 113.17, 111.74, 109.98, 109.86, 103.25, 100.88, 67.43, 65.68, 55.81, 53.88. LCMS: method 3, RT = 14.01; M + H^+: 541.30.

*Synthesis of Ethyl 2-(9H-Carbazol-4-yloxy)acetate (**17**).* A mixture of 4-hydroxycarbazole (1.90 g, 10.38 mmol), ethyl chloroacetate (1.11 mL, 10.38 mmol), and K_2CO_3 (1.43 g, 10.38 mmol) in acetone (150 mL) was stirred at 56 °C for 16 h. The solvent was removed under reduced pressure, and the residue was used in the next step with no further purification.

*Synthesis of 2-(9H-Carbazol-4-yloxy)acetic Acid (**18**).* A solution of **17** (0.72 g, 2.67 mmol) in THF (25 mL) was stirred with 1 M aqueous NaOH (20 mL, 20 mmol) at room temperature for 16 h. The reaction mixture was then acidified with 1 M HCl, and the organic layer was separated and concentrated under reduced pressure. The residue was triturated with ethyl acetate to give **18** as a colorless solid (0.16 g, 23%) and used in the next step with no further purification. ^{1}H NMR (DMSO 500 MHz): δ 11.27 (s, 1H), 8.24 (d, J = 7.8 Hz, 1H), 7.43 (d, J = 8.1 Hz, 1H), 7.32 (t, J = 7.6 Hz, 1H), 7.26 (t, J = 8.0 Hz, 1H), 7.13 (t, J = 7.5 Hz, 1H), 7.07 (d, J = 8.0 Hz, 1H), 6.57 (d, J = 8.0 Hz, 1H), 4.87 (s, 2H). LCMS: method 2: RT: 0.52 min; M + H^+: 242.03.

*Synthesis of 2-(9H-Carbazol-4-yloxy)-N-[2-(2-methoxyphenoxy)-ethyl]acetamide (**19**).* To a solution of **18** (0.075 g, 0.29 mmol), 2-(2-methoxyphenoxy)ethanamine (0.05 g, 0.29 mmol) and HOBt (0.054 g, 0.35 mmol) in anhydrous DMF (2 mL), EDC hydrochloride (0.068 g, 0.35 mmol), and DIPEA (0.15 mL, 0.88 mmol) were added, and the reaction was stirred at room temperature for 16 h. After this period, the solvent was removed under reduced pressure, and the residue was purified by flash column chromatography gradient elution of petroleum ether/ethyl acetate (90/10 to 0/100) to give **19** as a colorless solid (0.08 g, 64%). ^{1}H NMR ($CDCl_3$ 500 MHz): δ 8.22 (d, J = 7.8 Hz, 1H), 8.17 (br s, 1H), 7.51−7.38 (m, 2H), 7.34 (d, J = 7.5 Hz, 1H), 7.29 (t, J = 8.0 Hz, 1H), 7.10 (d, J = 8.1 Hz, 1H), 7.00 (t, J = 7.5 Hz, 1H), 6.97−6.92 (m, 1H), 6.91−6.84 (m, 1H), 6.78 (d, J = 7.9 Hz, 1H), 6.63 (d, J = 8.0 Hz, 1H), 4.81 (s, 2H), 4.15 (t, J = 5.1 Hz, 2H), 3.81 (q, J = 5.4 Hz, 2H), 3.50 (s, 3H). ^{13}C NMR ($CDCl_3$ 126 MHz): δ 168.85, 153.62, 141.03, 138.72, 131.74, 126.68, 125.27, 122.77, 122.32, 120.82, 119.88, 115.40, 111.89, 110.10, 104.89, 101.76, 68.64, 67.85, 55.42, 38.75. LCMS: method 3, RT = 19.52; M + H^+: 391.20.

*Synthesis of 2-(Oxiran-2-ylmethoxy)-9H-carbazole (**20**).* To a solution of 2-hydroxycarbazole (1.0 g, 5.46 mmol), NaOH (0.24 g, 6.0 mmol) in water (5 mL), a solution of 2-(bromomethyl)oxirane (0.70 mL, 8.19 mmol) in DMSO (1 mL) was added dropwise. The reaction mixture was stirred at 45 °C for 16 h. After cooling to room temperature, the resulting precipitate was filtered and triturated with isopropanol to give the desired compound **20** as a colorless solid (0.13 g, 9%). ^{1}H NMR ($CDCl_3$ 500 MHz): δ 8.02−7.90 (m, 3H), 7.41−7.31 (m, 2H), 7.21 (t, J = 7.4 Hz, 1H), 6.94 (s, 1H), 6.87 (d, J = 8.5 Hz, 1H), 4.31 (dd, J = 10.9, 3.1 Hz, 1H), 4.06 (dd, J = 10.9, 5.7 Hz, 1H), 3.42 (br s, 1H), 2.94 (t, J = 4.6 Hz, 1H), 2.86−2.76 (m, 1H). LCMS: method 1: RT: 0.60 min; M + H^+: 240.02.

*Synthesis of 1-(9H-Carbazol-2-yloxy)-3-[2-(2-methoxyphenoxy)-ethylamino]propan-2-ol (**21**).* A mixture of **20** (0.13 g, 0.56 mmol) and 2-(2-methoxyphenoxy)ethanamine (0.095 g, 0.56 mmol) in ethanol (15 mL) was stirred at 65 °C for 16 h. The solvent was removed under reduced pressure, and the residue was purified by flash column chromatography gradient elution of DCM/methanol (100/0 to 95/5). The compound obtained was further purified by flash column chromatography gradient elution of DCM/methanol = (100/0 to 90/20) to give **21** as a colorless solid (0.076 g, 33%). ^{1}H NMR (DMSO 600 MHz): δ 11.08 (s, 1H), 7.96 (d, J = 7.7 Hz, 1H), 7.93 (d, J = 8.5 Hz, 1H), 7.40 (d, J = 8.0 Hz, 1H), 7.29−7.23 (m, 1H), 7.11−7.06 (m, 1H), 6.97−6.92 (m, 3H), 6.89−6.82 (m, 2H), 6.76 (dd, J = 8.5, 2.2 Hz, 1H), 5.14−5.03 (m, 1H), 4.03−3.98 (m, 3H), 3.97−3.95 (m, 2H), 3.72 (s, 3H), 2.90 (t, J = 5.6 Hz, 2H), 2.79 (dd, J = 11.9, 3.9 Hz, 1H), 2.69 (dd, J = 11.8, 6.4 Hz, 1H); ^{13}C NMR (DMSO 151 MHz): δ 158.31, 149.59, 148.50, 141.48, 140.16, 124.56, 123.09, 121.47, 121.32, 121.16, 119.69, 118.96, 116.62, 114.01, 112.61, 111.04, 108.55, 95.63, 71.39, 68.77, 55.89, 52.93, 48.94; LCMS: method 3, RT = 12.59; M + H^+: 407.15.

*Synthesis of 9-(Oxiran-2-ylmethyl)carbazole (**22**).* KOH (0.20 g, 3.59 mmol) was added to a solution of 9*H*-carbazole (0.50 g, 2.99 mmol) in acetonitrile (5 mL), and the reaction mixture was stirred at room temperature for 1 h. Then, the reaction mixture was cooled in an ice bath, and 2-(bromomethyl)oxirane (0.64 mL, 7.48 mmol) was added dropwise. After the addition, the ice bath was removed, and the reaction mixture was stirred at room temperature for 20 h. After this period, the reaction mixture was partitioned between ethyl acetate and water, and the organic layer was washed with water and brine, dried over $MgSO_4$, filtered, and concentrated. The residue was triturated with hexane and recrystallized from ethyl acetate/hexanes to yield **22** as a colorless solid (0.48 g, 68%) and used in the next step with no further purification. ^{1}H NMR ($CDCl_3$ 500 MHz): δ 8.11 (dt, J = 7.8, 1.0 Hz, 2H), 7.53−7.45 (m, 4H), 7.31−7.24 (m, 2H), 7.27 (s, 2H), 4.64 (dd, J = 15.9, 3.4 Hz, 1H), 4.42 (dd, J = 15.9, 4.8 Hz, 1H), 3.38−3.35 (m, 1H), 2.82 (t, J = 4.4 Hz, 1H), 2.59 (dd, J = 4.8, 2.5 Hz, 1H); LCMS: method 2, RT = 3.03 min; M + H^+: 224.15.

*Synthesis of 1-Carbazol-9-yl-3-(2-phenylethylamino)propan-2-ol (**23**).* A solution of **22** (0.10 g, 0.43 mmol) and phenethylamine (0.05 mL, 0.43 mmol) in ethanol (5 mL) was stirred at 65 °C for 16 h. Then, the solvent was removed under reduced pressure, and the residue was purified by flash column chromatography gradient elution of petroleum ether/ethyl acetate = (100/0 to 0/100) to give **23** as a colourless oil (0.07 g, 49%). ^{1}H NMR (DMSO 600 MHz): δ 8.11 (d, J = 7.6 Hz, 2H), 7.57 (d, J = 8.2 Hz, 2H), 7.40 (t, J = 7.6 Hz, 2H), 7.26 (t, J = 7.5 Hz, 2H), 7.20 (d, J = 7.5 Hz, 2H), 7.16 (t, J = 7.4 Hz, 3H), 5.02 (s, 1H), 4.43 (dd, J = 14.8, 5.3 Hz, 1H), 4.24 (dd, J = 14.8, 6.7 Hz, 1H), 3.97 (p, J = 5.9 Hz, 1H), 2.77−2.66 (m, 4H), 2.60 (dd, J = 11.8, 4.9 Hz, 1H), 2.54 (dd, J = 11.8, 6.1 Hz, 1H). ^{13}C NMR (DMSO 151 MHz): δ 141.03, 140.92, 129.07, 128.67, 126.27, 125.93, 122.45, 120.47, 119.05, 110.17, 69.24, 53.46, 51.66, 47.48, 36.47. LCMS: method 3, RT = 12.76 min; M + H^+: 345.15.

*Synthesis of N-[2-(2-Methoxyphenoxy)ethyl]-2-morpholino-ethanamine (**24**).* A mixture of 4-(2-aminoethyl)morpholine (0.28 mL, 2.16 mmol), **3** (0.50 g, 2.16 mmol), and TEA (0.90 mL, 6.49 mmol) in THF (25 mL) was stirred at 65 °C for 4 h. After this time, the solvent was removed under reduced pressure, and the residue was purified by reverse phase chromatography gradient elution of water/methanol = 90/10 to 0/100 to give **24** as a colorless oil (0.055 g, 9%). ^{1}H NMR (DMSO 500 MHz): δ 7.03−6.90 (m, 2H), 6.88−6.82 (m, 2H), 3.96 (t, J = 5.6 Hz, 2H), 3.72 (s, 4H), 3.52 (t, J = 4.6 Hz, 4H), 2.83 (t, J = 5.5 Hz, 2H), 2.63 (t, J = 6.4 Hz, 2H), 2.36−2.29 (m, 6H). LCMS: method 1: RT: 0.39 min; M + H^+: 281.13.

*Synthesis of 1-(9H-Carbazol-4-yloxy)-3-[2-(2-methoxyphenoxy)-ethyl-(2-morpholinoethyl)amino]propan-2-ol (**25**).* A mixture of **24** (36.6 mg, 0.13 mmol) and **5** (30.6 mg, 0.13 mmol) in ethanol (15 mL) was stirred at 65 °C for 16 h. Then, the solvent was removed under reduced pressure, and the residue was purified by flash column chromatography gradient elution of petroleum ether/ethyl acetate =

DOI: 10.1021/acs.jmedchem.8b01325
J. Med. Chem. 2019, 62, 5312−5329

(100/0 to 0/100) to give **25** as a colorless oil (0.022 g, 29%). ^{1}H NMR ($CDCl_3$ 500 MHz): δ 8.28 (d, J = 7.7 Hz, 1H), 8.17 (s, 1H), 7.41−7.32 (m, 2H), 7.30 (t, J = 8.0 Hz, 1H), 7.18−7.15 (m, 1H), 7.02 (d, J = 8.0 Hz, 1H), 6.94−6.75 (m, 4H), 6.68 (d, J = 8.0 Hz, 1H), 4.35−4.28 (m, 1H), 4.23−4.18 (m, 2H), 4.09 (t, J = 5.6 Hz, 2H), 3.82 (s, 3H), 3.69 (t, J = 4.7 Hz, 4H), 3.18−3.03 (m, 3H), 3.00−2.91 (m, 2H), 2.89−2.79 (m, 1H), 2.67−2.39 (m, 6H). ^{13}C NMR ($CDCl_3$ 126 MHz): δ 155.28, 149.38, 148.11, 140.89, 138.70, 126.71, 124.86, 122.89, 122.62, 121.24, 120.83, 119.46, 113.13, 112.64, 111.69, 110.00, 103.58, 101.17, 69.56, 68.68, 67.40, 66.63, 57.56, 56.60, 55.73, 55.63, 53.20, 51.72. LCMS: method 3, RT = 12.76; M + H$^+$: 520.30.

Biology. *Animal Husbandry.* Tissues obtained from wildtype CD-1mice (Charles Rivers, UK) of either sex, at postnatal day 2 (P2), were used for the preparation of the mouse cochlear cultures that were then used for screening, live imaging with GTTR, and electrophysiology. Animals were raised according to Home Office guidelines, and all experiments were performed in accordance with the Home Office Animals (Scientific Procedures) Act 1986 and with approval of the Animal Welfare and Ethical Review Board at the University of Sussex.

Mouse Cochlear Culture Preparation. Cochlear cultures were prepared from CD-1 mice as previously described by Russell and Richardson.[28] In brief, P2 pups were killed by cervical dislocation and surface sterilized by three 1 min washes in 80% ethanol. Subsequent dissections were performed in Hanks buffered salt solution (HBSS; Thermo Shandon 14025050) buffered with 10 mM Hepes (Sigma H0887) (HBHBSS). Cochleae were removed from the bony labyrinth and explanted onto collagen-coated (Corning 354236) coverslips and immersed in rat cochlear culture media (RCM—93% DMEM-F12, 7% fetal bovine serum and 10 μg mL^{-1} ampicillin), sealed in Maximow slide assemblies, and left to adhere to the collagen for 24 h at 37 °C.

Mouse Cochlear Culture Protection Assay. Following 24 h incubation, coverslips with adherent cochleae were removed from the Maximow slide assemblies, placed in 35 mm Petri dishes (Greiner Bio-One 627161) and incubated for 48 h at 37 °C in a 5% CO_2 incubator in the presence of 1 mL RCM/DMEM-F12 (1:4) containing either vehicle (0.5% DMSO), 5 μM gentamicin (Sigma G3632), 5 μM gentamicin along with selected concentrations of the potentially protective compounds, or the potential protectants alone. Initially a dose−response experiment was run for the parent compound from which subsequent concentrations were selected. Following 48 h incubation, cultures were washed twice in phosphate-buffered saline, fixed in 3.7% formaldehyde (Sigma F1635), and stained with TRITC-phalloidin (Sigma P1951). Cultures were mounted on glass slides with Vectashield (Vector Laboratories H-1000) and imaged using a Zeiss Axioplan microscope, captured with a 40× objective (0.75 NA). Each screen was repeated 2−8 times.

Confocal Imaging. Confocal microscopy was used for high-resolution imaging of the mechanosensory hair bundles in order to assess any morphological disruption induced by the compounds of interest.

Slides were imaged on a Leica SP8 confocal microscope using the 561 nm laser (at 3% intensity) and a 100× 1.44 NA oil-immersion lens. Images were captured at a resolution of 736 × 400 pixels (and a zoom of ×2.0 with a ×4 line average) using a low detector gain (511) in order to reduce noise and improve image quality. Z-projections were created in ImageJ.

Quantification of OHC Survival. For quantification of HC survival, images from the mid-basal region were analyzed. Numbers of OHCs in a 300 μm long segment of the cochlea were counted at a position approximately 20% along the length of the cochlea from the basal end. The presence of a hair bundle was the criterion used as a marker of HC survival. Although HCs can survive without a bundle,[23,29] the latter is essential for sound transduction and provides a viable marker when searching for an otoprotectant. IHCs were not counted because of the lack of damage to this cell type caused by exposure to 5 μM gentamicin.

Electrophysiology on Mouse Cochlear Cultures. MET currents were recorded and analyzed using previously described methods.[20] In brief, OHCs in organotypic cultures prepared from P2 CD-1 mice were studied, with recordings performed in cultures that had been maintained for 1−2 days in vitro. MET currents were recorded using the whole-cell configuration of the patch clamp technique both before and during compound exposure at membrane potentials ranging from −164 to +96 mV. Currents were elicited by stimulating the OHC hair bundles using a fluid jet from a pipette (tip diameter 8−10 μm) driven by a piezoelectric disc.[7,30] Mechanical stimuli (filtered at 1.0 kHz, 8-pole Bessel) were applied as 45 Hz sinusoids with driver voltage amplitudes of ±40 V. Currents were acquired using pClamp (Molecular Devices) software and stored on computer for off-line analysis. For all recordings, series resistance compensation was applied (60−80%), and the average residual series resistance was calculated to be 1.37 ± 0.08 MΩ (n = 47). The average maximum MET current size was 1.50 ± 0.07 nA (n = 49), resulting in a maximum voltage drop across the residual series resistance of 2.1 mV, a value sufficiently small to not require any correction to quoted voltage values.

Dose response curves were fitted with the equation

$$\frac{I}{I_C} = \frac{1}{1 + ([B]/K_D)^{n_H}} \quad (1)$$

where I_C is the control current in the absence of the compound, [B] is the concentration of the blocking compound, K_D is the half-blocking concentration, and n_H is the Hill coefficient. Permeation and block of the MET channel for carvedilol and **13** were quantified by fitting a two barrier−one binding site model to the fractional block curves, as described in detail before.[20,31] This model is similar to that used to describe block of the MET currents by DHS[7] but modified to allow for Hill coefficients different from one.

Block of GTTR Loading into Mouse Cochlear Culture Hair Cells. Coverslips were removed from the Maximow slide assemblies, placed in a Perspex viewing chamber and immersed in 500 μL HBHBSS. Cultures were treated with either 100 μM carvedilol, 100 μM of the carvedilol derivative **13** or 1% DMSO as a control, with carvedilol and **13** being dissolved in this solvent. After 5 min incubation time at room temperature, GTTR was added at a final concentration of 0.2 μM, and incubation was continued for a further 10 min. The culture was washed three times with HBHBSS before live imaging on a Zeiss Axioplan2 microscope. A 60× water immersion lens was used to take images of both the apical and basal regions of the cochlea across a time range from 14 to 24 min post-GTTR application. Three repeats were conducted. For quantification, analysis was performed on images from the mid-basal region, 24 min post-GTTR application. Ten cells from the first row of OHCs central to the 1200 pixel image were analyzed, as shown by the asterisk in Figure 16, obtaining intensity values from a 40 × 40 pixel region of interest (ROI). Three background ROIs were measured, averaged, and subtracted from each individual cell value, which were then averaged and repeated across three trials. One background ROI was taken from nonsensory HC cellular space to account for any endocytic loading.

Statistics. All graphical representations display mean ± standard error of the mean. Numbers above bars denote the number of independent experimental replicates. One-way ANOVA was applied followed by Tukey's multiple comparison test, assuming normal distribution of the data. For GTTR live imaging experiments, an unpaired t-test was used. Significance was set at * = $p < 0.05$, ** = $p < 0.01$, and *** = $p < 0.001$.

■ ASSOCIATED CONTENT

Supporting Information

The Supporting Information is available free of charge on the ACS Publications website at DOI: 10.1021/acs.jmedchem.8b01325.

Molecular formula strings (CSV)

Protection of carvedilol and compound 13 in zebrafish lateral line; antimicrobial activity of gentamicin in the

DOI: 10.1021/acs.jmedchem.8b01325
J. Med. Chem. 2019, 62, 5312−5329

presence of carvedilol and compound 13; supplemental methods zebrafish animal husbandry and screening for otoprotection; bacterial growth conditions and antimicrobial drug susceptibility testing (PDF)

AUTHOR INFORMATION

Corresponding Author

*E-mail: m.derudas@sussex.ac.uk. Phone: +44(0)1273876591.

ORCID

Marco Derudas: 0000-0003-1731-2855

Author Contributions

⊥M.O. and N.K.K. contributed equally to the work in this manuscript.

Notes

The authors declare no competing financial interest.

ACKNOWLEDGMENTS

This work was supported by the Medical Research Council (MR/K005561/1 to C.J.K., G.P.R., and S.E.W.). All data are provided in the Results, and the Experimental Section of the paper and in the Supporting Information.

ABBREVIATIONS

MET, mechanoelectrical transducer; AG, aminoglycoside; ROS, reactive oxygen species; OHC, outer hair cell; IHC, inner hair cell; DMF, dimethylformamide; TEA, tryethylamine; HOBt, 1-hydroxybenzotriazole; EDC, *N*-(3-dimethylaminopropyl)-*N*′-ethylcarbodiimide; DIPEA, *N*,*N*-diisopropylethylamine; GTTR, gentamicin Texas red; SAR, structure−activity relationship; DHS, dihydrostreptomycin; THF, tetrahydrofuran; DMC, dichloromethane.

REFERENCES

(1) Avent, M. L.; Rogers, B. A.; Cheng, A. C.; Paterson, D. L. Current use of aminoglycosides: indications, pharmacokinetics and monitoring for toxicity. *Intern. Med. J.* **2011**, *41*, 441−449.

(2) Prayle, A.; Smyth, A. R. Aminoglycoside use in cystic fibrosis: therapeutic strategies and toxicity. *Curr. Opin. Pulm. Med.* **2010**, *16*, 604−610.

(3) Horsburgh, C. R., Jr.; Barry, C. E., III; Lange, C. Treatment of tuberculosis. *N. Engl. J. Med.* **2015**, *373*, 2149−2160.

(4) Rizzi, M. D.; Hirose, K. Aminoglycoside ototoxicity. *Curr. Opin. Otolaryngol. Head Neck Surg.* **2007**, *15*, 352−357.

(5) Hashino, E.; Shero, M. Endocytosis of aminoglycoside antibiotics in sensory hair cells. *Brain Res.* **1995**, *704*, 135−140.

(6) Gale, J. E.; Marcotti, W.; Kennedy, H. J.; Kros, C. J.; Richardson, G. P. FM1-43 dye behaves as a permeant blocker of the hair-cell mechanotransducer channel. *J. Neurosci.* **2001**, *21*, 7013−7025.

(7) Marcotti, W.; Van Netten, S. M.; Kros, C. J. The aminoglycoside antibiotic dihydrostreptomycin rapidly enters mouse outer hair cells through the mechano-electrical transducer channels: aminoglycoside entry into hair cells. *J. Physiol.* **2005**, *567*, 505−521.

(8) Wang, Q.; Steyger, P. S. Trafficking of systemic fluorescent gentamicin into the cochlea and hair cells. *J. Assoc. Res. Otolaryngol.* **2009**, *10*, 205−219.

(9) Alharazneh, A.; Luk, L.; Huth, M.; Monfared, A.; Steyger, P. S.; Cheng, A. G.; Ricci, A. J. Functional hair cell mechanotransducer channels are required for aminoglycoside ototoxicity. *PLoS One* **2011**, *6*, No. e22347.

(10) Owens, K. N.; Coffin, A. B.; Hong, L. S.; Bennett, K. O. C.; Rubel, E. W.; Raible, D. W. Response of mechanosensory hair cells of the zebrafish lateral line to aminoglycosides reveals distinct cell death pathways. *Hear. Res.* **2009**, *253*, 32−41.

(11) Coffin, A. B.; Rubel, E. W.; Raible, D. W. Bax, Bcl2, and p53 differentially regulate neomycin- and gentamicin-induced hair cell death in the zebrafish lateral line. *J. Assoc. Res. Otolaryngol.* **2013**, *14*, 645−659.

(12) Coffin, A. B.; Williamson, K. L.; Mamiya, A.; Raible, D. W.; Rubel, E. W. Profiling drug-induced cell death pathways in the zebrafish lateral line. *Apoptosis* **2013**, *18*, 393−408.

(13) Jiang, M.; Karasawa, T.; Steyger, P. S. Aminoglycoside-induced cochleotoxicity: a review. *Front. Cell. Neurosci.* **2017**, *11*, 308.

(14) O'Sullivan, M. E.; Perez, A.; Lin, R.; Sajjadi, A.; Ricci, A. J.; Cheng, A. G. Towards the prevention of aminoglycoside-related hearing loss. *Front. Cell. Neurosci.* **2017**, *11*, 325.

(15) Jensen-Smith, H. C.; Hallworth, R.; Nichols, M. G. Gentamicin rapidly inhibits mitochondrial metabolism in high-frequency cochlear outer hair cells. *PLoS One* **2012**, *7*, No. e38471.

(16) Huth, M. E.; Han, K.-H.; Sotoudeh, K.; Hsieh, Y.-J.; Effertz, T.; Vu, A. A.; Verhoeven, S.; Hsieh, M. H.; Greenhouse, R.; Cheng, A. G.; Ricci, A. J. Designer aminoglycosides prevent cochlear hair cell loss and hearing loss. *J. Clin. Invest.* **2015**, *125*, 583−592.

(17) Duscha, S.; Boukari, H.; Shcherbakov, D.; Salian, S.; Silva, S.; Kendall, A.; Kato, T.; Akbergenov, R.; Perez-Fernandez, D.; Bernet, B.; Vaddi, S.; Thommes, P.; Schacht, J.; Crich, D.; Vasella, A.; Böttger, E. C. Identification and evaluation of improved 4′-O-(alkyl) 4,5-disubstituted 2-deoxystreptamines as next-generation aminoglycoside antibiotics. *mBio* **2014**, *5*, No. e01827.

(18) Avent, M. L.; Rogers, B. A.; Cheng, A. C.; Paterson, D. L. Current use of aminoglycosides: indications, pharmacokinetics and monitoring for toxicity: aminoglycosides: review and monitoring. *Intern. Med. J.* **2011**, *41*, 441−449.

(19) Kamogashira, T.; Fujimoto, C.; Yamasoba, T. Reactive oxygen species, apoptosis, and mitochondrial dysfunction in hearing loss. *BioMed Res. Int.* **2015**, *2015*, 1.

(20) Kirkwood, N. K.; O'Reilly, M.; Derudas, M.; Kenyon, E. J.; Huckvale, R.; van Netten, S. M.; Ward, S. E.; Richardson, G. P.; Kros, C. J. d-Tubocurarine and berbamine: alkaloids that are permeant blockers of the hair cell's mechano-electrical transducer channel and protect from aminoglycoside toxicity. *Front. Cell. Neurosci.* **2017**, *11*, 262.

(21) Kenyon, E. J.; Kirkwood, N. K.; Kitcher, S. R.; O'Reilly, M.; Derudas, M.; Cantillon, D. M.; Goodyear, R. J.; Secker, A.; Baxendale, S.; Bull, J. C.; Waddell, S. J.; Whitfield, T. T.; Ward, S. E.; Kros, C. J.; Richardson, G. P. Identification of ion-channel agonists/antagonists that protect against aminoglycoside-induced hair-cell death. *J. Clin. Invest. Insight* **2017**, *2*, No. e96773.

(22) Ou, H. C.; Cunningham, L. L.; Francis, S. P.; Brandon, C. S.; Simon, J. A.; Raible, D. W.; Rubel, E. W. Identification of FDA-approved drugs and bioactives that protect hair cells in the zebrafish (danio rerio) lateral line and mouse (mus musculus) utricle. *J. Assoc. Res. Otolaryngol.* **2009**, *10*, 191−203.

(23) Majumder, P.; Moore, P. A.; Richardson, G. P.; Gale, J. E. Protecting mammalian hair cells from aminoglycoside-toxicity: assessing phenoxybenzamine's potential. *Front. Cell. Neurosci.* **2017**, *11*, 94.

(24) Chowdhury, S.; Owens, K. N.; Herr, R. J.; Jiang, Q.; Chen, X.; Johnson, G.; Groppi, V. E.; Raible, D. W.; Rubel, E. W.; Simon, J. A. Phenotypic optimization of urea−thiophene carboxamides to yield potent, well tolerated, and orally active protective agents against aminoglycoside-induced hearing loss. *J. Med. Chem.* **2018**, *61*, 84−97.

(25) Ba Huy, P. T.; Manuel, C.; Meulemans, A.; Sterkers, O.; Amiel, C. Pharmacokinetics of gentamicin in perilymph and endolymph of the rat as determined by radioimmunoassay. *J. Infect. Dis.* **1981**, *143*, 476−486.

(26) Wyman, J.; Gill, S. J. *Binding and Linkage: Functional Chemistry of Biological Macromolecules*; University Science Books: Mill Valley, CA, 1990.

(27) Steyger, P. S.; Peters, S. L.; Rehling, J.; Hordichok, A.; Dai, C. F. Uptake of gentamicin by bullfrog saccular hair cells in vitro. *J. Assoc. Res. Otolaryngol.* **2003**, *4*, 565−578.

DOI: 10.1021/acs.jmedchem.8b01325
J. Med. Chem. 2019, 62, 5312−5329

(28) Russell, I. J.; Richardson, G. P. The morphology and physiology of hair cells in organotypic cultures of the mouse cochlea. *Hear. Res.* **1987**, *31*, 9−24.
(29) Gale, J. E.; Meyers, J. R.; Periasamy, A.; Corwin, T. Survival of bundleless hair cells and subsequent bundle replacement in the bullfrog's saccule. *J. Neurobiol.* **2002**, *50*, 81−92.
(30) Kros, C. J.; Rüsch, A.; Richardson, G. P. Mechano-electrical transducer currents in hair cells of the cultured neonatal mouse cochlea. *Proc. R. Soc. London, Ser. B* **1992**, *249*, 185−193.
(31) van Netten, S. M.; Kros, C. J. Insights into the pore of the hair cell transducer channel from experiments with permeant blockers. *Curr. Top. Membr.* **2007**, *59*, 375−398.

DOI: 10.1021/acs.jmedchem.8b01325
J. Med. Chem. 2019, 62, 5312−5329